Short-term effects of increased CO2, nitrate and temperature on photosynthetic activity in Ulva rigida (Chlorophyta) estimated by different pulse amplitude modulated fluorometers and oxygen evolution

F. L. Figueroa, J. Bonomi-Barufi, P. S. M. Celis-Plá, U. Nitschke, F. Arenas, S. Connan, M. H. Abreu, E.-J. Malta, R. Conde-Álvarez, F. Chow, et al.

Journal of Experimental Botany
February 2021, Volume 72, Issue 2, Pages 491-509
https://doi.org/10.1093/jxb/eraa473
https://archimer.ifremer.fr/doc/00655/76682/

Short-term effects of increased CO2, nitrate and temperature on photosynthetic activity in *Ulva rigida* (Chlorophyta) estimated by different pulse amplitude modulated fluorometers and oxygen evolution

Figueroa F L [1, *], Bonomi-Barufi J [2], Celis-Plá P S M [3, 4], Nitschke U [5], Arenas F [6], Connan S [7, 8], Abreu M H [9], Malta E-J [10], Conde-Álvarez R [1], Chow F [11], Mata M T [12], Meyerhoff O [13], Robledo D [14], Stengel D B [5]

[1] Malaga University. Institute of Blue Biotechnology and Development (IBYDA), Ecology Department, Faculty of Sciences, Campus Universitario de Teatinos s/n, Malaga, Spain
[2] Botany Departament, Federal University of Santa Catarina. Campus Trindade s/n, Florianópolis, SC, Brazil
[3] Laboratory of Costal Environmental Research,Center of Advances Studies. University of Playa Ancha. Traslaviña, Viña del Mar, Chile
[4] HUB AMBIENTAL UPLA, Vicerrectoría de Investigación, Postgrado e Innovación, Universidad de Playa Ancha, Valparaíso, Chile
[5] Botany and Plant Science, School of Natural Sciences, Ryan Institute for Environmental, Marine and Energy Research, National University of Ireland Galway, Galway, Ireland
[6] CIIMAR/CIMAR - Interdisciplinary Centre of Marine and Environmental Research, University of Porto, Rua dos Bragas, Porto, Portugal
[7] CNRS, GEPEA, UMR6144, Boulevard de l'Université, CRTT BP 406, 44602 Saint Nazaire Cedex, France
[8] Univ Brest, CNRS, IRD, Ifremer, LEMAR, Plouzane, France
[9] ALGAplus Ltd – R&D Department, Rua António Castilho, Angeja, Portugal
[10] Centro IFAPA Agua del Pino, Crtra. El Rómpido – Punta Umbría, Cartaya (Huelva), Spain
[11] Department of Botany, University of São Paulo, Rua do Matão, São Paulo, SP, Brazil
[12] Centro de Bioinnovación Antofagasta (CBIA), Faculty of Marine Sciences and Biological Resources, Antofagasta University, Antofagasta, Chile
[13] Heinz Walz GmbH Eichenring, Effeltrich, Germany
[14] CIVESTAV-IPN, Unidad Mérida Km6 Antigua Carretera a Progreso Apartado Postal, Cordemex, Mérida, Yucatán, México

* Corresponding author : F. L. Figueroa, email address : felix_lopez@uma.es

Abstract :

Short-term effects of pCO2 (700 – 380 ppm; HC-LC) and nitrate content (50-5 βM; HN-LC) on photosynthesis, estimated by different pulse amplitude modulated (PAMs) fluorometers and by oxygen evolution, were investigated in Ulva rigida (Chlorophyta) under solar radiation (ex-situ) and in the laboratory under artificial light (in-situ). After 6-days of incubation at ambient temperature (AT), algae were subjected to a 4 oC-temperature increase (AT+4oC) for 3 d. Both in-situ and ex-situ, maximal electron

transport rate (ETRmax) and in situ gross photosynthesis (GP) measured by O2 evolution presented the highest values under HCHN, and the lowest under HCLN, across all measuring systems. Maximal quantum yield (Fv/Fm), and ETRmax of PSII (ETR(II)max) and of PSI (ETR(I)max), decreased under HCLN under AT+4°C. Ex situ ETR was higher than in situ ETR. At noon, Fv/Fm decreased (indicating photoinhibition), whereas ETR(II)max and maximal non-photochemical quenching (NPQmax) increased. ETR(II)max decreased under AT+4oC in contrast to Fv/Fm, photosynthetic efficiency (αETR) and saturated irradiance (EK). Thus, U. rigida exhibited a decrease in photosynthetic production under acidification, LN levels and AT+4oC. These results emphasize the importance of studying the interactive effects between environmental parameters using in-situ vs. ex-situ conditions when aiming to evaluate the impact of global change on marine macroalgae.

Keywords : Acidification, climate change, electron transport rates, in vivo chlorophyll a fluorescence, nitrate, photosystem I and II, temperature

Abbreviations

A Absorptance

AT Ambient temperature

ETR Electron transport rate

Fv/Fm Maximal quantum yield

HC High pCO_2 (700 ppm)

HN High nitrate levels (50 μM)

LC Low pCO_2 (380 ppm)

LN Low nitrate levels (5 μM)

NPQ Non photochemical quenching

PAM Pulse amplitude modulated

PAR Photosynthetic active radiation

PSI Photosystem I

PSII Photosystem II

RLC Rapid light curves

Y(II) Effective quantum yield

INTRODUCTION

Ocean acidification will increase by 0.3–0.4 pH unit by 2100 due to the anticipated rise in atmospheric CO_2 levels to 800–1000 ppm by the end of this century, according to the 'business-as-usual' CO_2 emission scenario (Caldeira and Wickett, 2003). This acidification process may significantly change the water carbonate chemistry (Hall-Spencer et al., 2008; Pelejero et al., 2010) and then affect not only calcifying organisms (Riebesell et al., 2000) but also non-calcifying photoautotrophs (Roleda et al., 2012). So far, the cumulative effects of climatically realistic CO_2-driven pH change on non-calcifying seaweeds remain poorly understood (Kroeker et al., 2010). Studies on the ecological and physiological impacts of elevated CO_2 concentrations on macroalgae were initiated in the early 1990s: growth of *Porphyra yezoensis* juveniles was significantly enhanced in cultivation enriched with CO_2 up to 1000 ppmv (Gao et al., 1991). Macroalgae are a highly diverse group with complex functional morphologies and varied ecological roles. Morphological plasticity, in addition to physiological mechanisms, may further determine the algal capacity to acclimate to global change scenarios (Falkenberg et al., 2013; Gao et al., 2018, 2019). In macroalgae, doubling CO_2 level caused an increase in photosynthetic activity of 52-130% depending on the species (Riebesell et al., 2007; Ní Longphuirt et al., 2013; Celis-Plá et al., 2015), but the magnitude of the effects of a CO_2 increase can be related to the presence or absence of a carbon concentration mechanism (CCM). Since *Ulva* spp. species possess carbon concentration mechanismsor incorporate bicarbonate directly through an anion exchanger (AE) system (Axelsson et al., 1995), the effects of a CO_2 increase on their photosynthetic capacity can be expected to be moderate.

Moreover, studies on the effect of climate change on aquatic organisms have mostly been conducted applying only one or two variables, and interactions among multiple factors have been studied only scarcely (Gordillo et al., 2001; Gao et al., 2018). The sensitivity of algae to acidification is also expected to be complex, due to interactive effects of pH and CO_2 on photosynthesis. Although elevated seawater CO_2 concentrations may enhance photosynthetic and growth rates (particularly in species without carbon concentrating mechanisms), such increase may be limited by nutrient availability (Raven et al., 2005; Stengel et al., 2014; Li et al., 2018). Photosynthesis, nutrient uptake, growth, and other metabolic processes are affected by temperature, light and nutrient availability, and seasonal changes in these parameters are further likely to interact with CO_2 effects on the algal metabolism (Tyrrell et al., 2008; Martin and Gattuso, 2009; Mercado and Gordillo, 2011; Brodie et al., 2014). Therefore, outdoor mesocosm studies (*in situ* measurements) are particularly useful for

monitoring CO_2 impacts over time capturing natural temperature, nutrient and light fluctuations (Celis-Plá et al., 2017a, b).

The mechanisms for algal acclimatization to climate change have been evaluated through the effect on photoinhibition, photoprotection, nutrient uptake systems and patterns of growth, reproduction and morphogenesis of different developmental stages of macroalgae (Villafañe et al., 2003; Celis-Plá et al., 2016; Gao et al., 2019). Short-term (<1 year) experiments have been performed and reveal mixed responses, depending on algal species tested and culture conditions applied (Porzio et al., 2011; Cornwall et al., 2012; Figueroa et al., 2014a, b, c). Recently, long term studies on the impact of acidification were also conducted in mesocosms in which the target pCO_2 was controlled via direct analysis of pCO_2 in seawater (Sordo et al., 2016).

The aim of this study was to evaluate the short-term (six days) impact of increasing pCO_2 on photosynthetic responses of the marine macroalga *Ulva rigida* (Chlorophyta) which is locally dominant on Mediterranean coasts. This study simulated a range of a global change scenarios under different nitrogen levels provided through nitrate pulses (high nitrate level *vs.* low nitrate level), comparable to elevated nitrogen supply from urban wastewaters (Bermejo et al., 2013). The high capacity of nutrient biofiltration of *Ulva* species can provide ecological services both in the coastal areas and in aquaculture systems. Therefore, it is critical to evaluate the likely effects of climate change on the physiology and biomass productivity of this species through the simulation of anticipated future conditions. The Mediterranean Sea is recognised as a priority area for climate studies due to the previously reported increases in average seawater temperature and the occurrence of heat extremes by 200 to 500% (Diffenbaugh et al., 2007; Mieszkowska et al., 2008; Louanchi et al., 2009).

This study was conducted in the frame of the Group of Aquatic Primary production (GAP) at the workshop "Influence of the pulsed-supply of nitrogen on primary productivity in phytoplankton and marine macrophytes: an experimental approach". *In situ* photosynthesis under solar radiation measured using Diving PAM (Stengel et al., 2014) and a Monitoring-PAM (Figueroa et al., 2014a) were previously published. Here, we provide additional data from the same experiment on *in vivo* chlorophyll fluorescence of PSII (maximal quantum yield, electron transport rate and non-photochemical quenching) under laboratory conditions (*ex situ*, artificial light) by using additional fluorometers: a Mini-PAM and a Dual-PAM. The latter fluorometer determines yield and electron transport rate of both PSI and PSII. Previous studies have shown that electron transport rate (ETR) can be used as an estimator of photosynthetic capacity, showing higher *in situ* fluorescence values under solar radiation than

under artificial light in laboratory (Longstaff et al., 2002; Jerez et al., 2016). Thus, a comparison of *in situ* versus *ex situ* measurements is key to identifying an appropriate and reliable protocol to estimate algal photosynthetic activity. The value of applying different approaches in the determination of photosynthesis in *Ulva rigida* under different CO_2, nitrate and temperature conditions is also discussed.

MATERIAL AND METHODS

Algae and experimental design

Ulva rigida C. Agardh (Chlorophyta) was collected at La Araña Beach (Malaga, Southern Iberian Peninsula, Spain) (Fig. 1A-D). *U. rigida* is a two-cell layer laminar macroalga, characterized by a rapid growth and nitrophilic pattern.

The algae were transported to the laboratory in an icebox, cleaned from epibionts and acclimated during four days to low Carbon (C) and low Nitrate (N) conditions prior to experimental exposure. The experimental design is described in detail in Stengel et al. (2014). Briefly, the algal species was cultivated in a mesocosm system at two CO_2 levels, *i.e.* high (HC, 700 ppm) and low CO_2 (LC, 380 ppm), and two nitrate levels, *i.e.* high (HN, 50 μM) and low nitrate (LN, 5 μM). Nitrate was added as KNO_3. Phosphate as K_3PO_4 (1 μM) was added daily in both LN and HN treatments to avoid any phosphate limitation. The experiment was conducted at the Grice-Hutchinson experimental centre of Malaga University (Fig. 1E). The experimental system was composed of 3 open vessels (0.094 m^2 surface area, 14 L volume) per treatment, each vessel being considered as a replicate unit (Fig. 1F-G). Each vessel was connected independently to a 60-L tank (header tank), the water flow rate between both being 0.84 ±0.05 L min^{-1}, representing a turnover rate of 26±1% h^{-1}. The open vessels were located within 1000-L tanks with circulating fresh water permanently cooled by two cooling units Titan-500 (Aqua Medic GmbH, Bissendorf, Germany) in order to maintain the temperature, as reported by Stengel et al. (2014).

The chosen low CO_2 level (380 ppm) falls within the range of surface pCO_2 in the Alborán Sea (367-394 ppm of pCO_2), according to McElhany and Busch (2013). This region is characterized as oligotrophic, with maximum nitrate level reaching 5 μM at certain periods of the year (Ramírez et al., 2005). Thus, the LCLN treatment was considered a control treatment, being closest to natural conditions. In addition to the different C and N treatments, after a 6-days, the algae were subjected to a 4°C temperature increase (AT+4^{o}C) relative to ambient temperature (AT) for a further three days.

Photosynthetic performance estimated by *in vivo* chlorophyll *a* fluorescence was determined using two different fluorometers, a Mini-PAM and a Dual-PAM (Walz, Effeltrich, Germany). In the case of the Mini-PAM, data were assessed at three different periods throughout the day: morning (M; 7:00-8:00 GMT), noon (N; 11:30-12:30 GMT) and evening (E; 17:00-18:00 GMT). Data were collected at two different days under each temperature condition, representing a total of six measurements per condition (n=6). The samples were transported under dark conditions from the out-door vessels to the laboratory (25 m distance), where the samples were kept for 15 min in darkness. Fluorescence parameters were then determined under *ex-situ* conditions in the laboratory. In the case of the Dual-PAM, data were measured only at the morning (M; 7:00-8:00 GMT, three times) and evening (E; 17:00-18:00 GMT, two times) periods. Data were collected at two different days only after temperature increase (AT+4°C). To allow statistical analyses, as a different number of measurements were conducted at each daytime, all data were pooled by period, and time was not considered as a factor, for a total of ten measurements per treatment (n=10).

The data produced by the Mini-PAM and Dual-PAM are compared to previous reported *in situ* data (under solar radiation) using a Diving-PAM (Stengel et al., 2014) and a Monitoring-PAM (Figueroa et al., 2014a).

In vivo chlorophyll *a* fluorescence of PSII using a Mini-PAM

Maximum quantum yield (F_v/F_m) was determined according to Schreiber et al. (1986) using the fluorometer Mini-PAM (Walz GmbH, Germany). After 15 min of dark acclimation, rapid light curves (RLC) were conducted. Following an initial quasi-dark measurement (~1.5 µmol photons m^{-2} s^{-1}) to provide estimates of minimum fluorescence (F_o), a saturating flash of 0.8 s with intensity of > 4000 µmol photons m^{-2} s^{-1} was applied to obtain the maximum fluorescence level from fully reduced PSII reaction centres (F_m) and F_v/F_m was obtained, with $F_v=F_m-F_o$.

Effective quantum yield of PSII (Y(II)) of algae under different actinic lights were calculated by formula (1) according to Genty et al. (1989), that is equivalent to $\Delta F/F_m'$ or ϕ_{II} (Kromkamp and Forster, 2003):

$$Y(II) = (F_m' - F) / F_m' \quad (1)$$

With F_m' being the maximum fluorescence in light induced by a saturating pulse, and F the fluorescence under actinic light. Y(II) was used to calculate the ***electron transport rate*** of PSII (ETR(II)), as shown in equation (2):

$$\text{ETR(II)}\ [\mu\text{mol electrons m}^{-2}\ \text{s}^{-1}] = \text{Y(II)} \times E_{PAR} \times \text{A} \times \text{F}_{II} \quad (2)$$

Where E_{PAR} is the incident irradiance of PAR (Photosynthetically Active Radiation, λ =400-700 nm), A is the absorptance, and F_{II} is the fraction of cellular chlorophyll *a* associated with LHCII (Light Harvesting Complex associated to PSII); 0.5 being the value for green algae (Grzymski et al., 1997). Although variation in F_{II} due to light conditions has been demonstrated, such changes were lower in green macroalgae than in other algal groups (Grzymski et al., 1997; Johnsen and Sakshaug, 2007); in our study, the value of F_{II} was considered as a constant. Absorptance was determined as A = 1 – T as reported by Figueroa et al. (2009). T is the transmittance estimated as shown in equation (3):

$$T = E_t / E_o \quad (3)$$

Where E_o is the incident irradiance of a high pressure lamp determined by a cosine corrected sensor Li-189 (LI-COR Ltd, Nebraska, USA) connected to a radiometer Li-250 (LI-COR Ltd, Nebraska, USA), and E_t is the transmitted irradiance, measured by placing a small thallus piece above the PAR sensor (Figueroa et al., 2009). Reflectance was not determined in this study since according to other reports, the reflectance of *Ulva* sp. measured by using integrating sphere, opal glass or other techniques, was very low, *i.e*. 0.04-0.06 (Mercado et al., 1996; Figueroa et al., 2003a). ETR values in *U. rigida* were then overestimated by only 4-6%.

Rapid light curves (RLC, ETR *vs.* irradiance curves) were conducted using 20-s exposure to eight incremental irradiances (53, 157, 300, 473, 686, 971, 1241 and 1640 µmol photons m^{-2} s^{-1}) of actinic red light. Light curves were fitted according to different models (Jassby and Platt, 1976; Platt and Gallegos, 1980; Eilers and Peters, 1988) to obtain the maximum ETR (ETR_{max}), the initial slope of the curves (α_{ETR}) and the irradiance of ETR saturation (E_k). The proportions of absorbed irradiance at ETR_{max} used as electron transport (E_{YII}) and energy dissipation (E_{YNPQ}, E_{YNO}) were calculated according to Hendrickson et al. (2004).

The energy dissipated as non-photochemical quenching

Yield of losses, Y(NO) and Y(NPQ), were determined according to Kramer et al. (2004a) and Hendrickson et al. (2004). Y(NO) is the fraction of energy passively dissipated as heat and fluorescence, mainly due to closed PSII reaction centres. High values indicate an inability of the macroalga to protect itself against photodamage by an excess of radiation. Y(NO) was calculated as in equation (4):

$$Y(NO) = F_t/F_m \quad (4)$$

Y(NPQ) is the fraction of energy dissipated as heat via regulated photoprotective mechanisms. High values are indicative of photoprotection capacity, and this parameter was calculated according to equation (5):

$$Y(NPQ) = (F_t/F_m') - Y(NO) \quad (5)$$

Considering that the sum of the three yield components (Y(II), Y(NO) and Y(NPQ)) adds up to 1, *i.e.* the total absorbed energy by the algal tissues, it was possible to determine the amount of energy used in photochemistry and the dissipated energy according to Hendrickson et al. (2004). The values of Y(II), Y(NPQ) and Y(NO) were obtained from the rapid light curves, considering the samples incubated at each actinic light for 20 s. These values were used to calculate the energy destined to each route by multiplying them by the absorbed PAR. This allowed the calculation of $E_{Y(II)}$, $E_{Y(NO)}$ and $E_{Y(NPQ)}$. These values were calculated at each absorbed PAR and are presented to illustrate the rates of energy destination.

Non-photochemical quenching (NPQ), as the expression of total energy dissipation, was calculated according to the ratio of both yield losses, which is similar to Stern-Volmer NPQ parameter (Bilger et al., 1995) as follows (equation 6):

$$NPQ = Y(NPQ)/Y(NO) = (F_m - F_m')/F_m \quad (6)$$

NPQ was calculated after each saturating pulse during the RLCs, and NPQ *vs*. irradiance relationships were determined. These curves were then fitted to different models (Jassby and Platt 1976; Platt and Gallegos, 1980; Eilers and Peters, 1988), allowing the calculation of

maximum NPQ values (NPQ_{max}); high NPQ values indicated a high capacity for acclimation to increased irradiance.

In vivo chlorophyll *a* fluorescence of PSI and PSII using a Dual PAM

All measurements were carried out using a Dual PAM-100 instrument (Walz, Effeltrich, Germany). Weak modulated measuring light from a 620 nm light emitting diode (LED) and blue actinic light of 250 μmol photons m^{-2} s^{-1} from 460 nm LED arrays were delivered to the upper algal surface by a DUAL-DR measuring head. Saturating light pulses of 300 ms duration and 10000 μmol photons m^{-2} s^{-1} intensity from 620 nm LED arrays were given simultaneously to the upper and lower algal side by the DUAL-DR and a DUAL-E emitter unit, respectively. The oxidation/reduction status of PSI reaction centres was followed by changes in the absorbance at 830 nm (Schreiber et al., 1988). For this purpose, 830 nm sample and 875 nm reference beams, both emitted by the DUAL-E unit, were passed through the alga and received by a photodiode located in the DUAL-DR measuring head. Both the DUAL-DR and the DUAL-E units were placed into a leaf holder (DUAL-B, Walz) in which Perspex rods guided the light between the alga and measuring units.

Experiments were carried out using the automated routine provided by the Dual-PAM software, with repetitive application of saturation pulses for assessment of fluorescence and P700 parameters, from which the quantum yields of PSI and PSII were derived by the software (Klughammer and Schreiber, 1994). Firstly, using low-light acclimated algae, the basal fluorescence was established and subsequently the F_m fluorescence was determined by the saturation pulse method. Secondly, the maximal P700 signal was determined by application of a saturation pulse after far-red pre-illumination. It is assumed that under donor-side limited conditions (produced by far-red exposure), a saturation pulse transiently induces full P700 oxidation. Briefly after the saturation pulse the minimum P700 signal is measured when P700 is fully reduced. The difference in signal between the fully reduced and oxidized states is denoted by P_m. Actinic illumination was started, and then saturation pulses were applied every 20 s, with the same pulses used for both fluorescence and P700 analyses. Twelve incremental irradiances were applied: 28, 40, 53, 100, 163, 211, 342, 522, 796, 1209, 1844, 2745 μmol photons m^{-2} s^{-1}. Each saturation pulse was followed by a 1-s dark-period to determine the minimal P700 signal level P_o (P700 fully reduced). Values for F and F_m' were recorded immediately before and during each saturation pulse, according to Oxborough and Baker (1997). P700 was measured in the dual-wavelength mode (photodetector set to

measure 875 nm and 830 nm pulse modulated light) (Schreiber and Klughammer, 2008). The P700 signal (P) was recorded just before a saturation pulse; then, briefly after onset of a saturation pulse (P_m) when maximum P700 oxidation under the effective experimental conditions is observed; and, finally, at the end of the 1-s dark interval following each saturation pulse (P_o determination). The P and P_m signals are referenced against P_o. In this way, unavoidable signal drifts, e.g. due to changes in the water status, do not disturb the actual measurements of P700 parameters.

The photosynthetic electron transport rates of PSI (ETR(I)) were calculated as follows (equation 7):

$$\text{ETR(I)}\ [\mu\text{mol electrons m}^{-2}\ \text{s}^{-1}] = \text{Y(I)} \times E_{PAR} \times \text{A} \times \text{F}_\text{I} \qquad (7)$$

where Y(I) is the effective quantum yield of PSI, E_{PAR} the incident irradiance of PAR, A the absorptance in the PAR region and F_I the fraction of chlorophyll *a* related to PSI. F_I was calculated as $F_I = 1 - F_{II}$ according to the F_{II} values of 0.5.

Photosynthetic parameters related to PSII were also obtained using the Dual PAM, and calculations of $Y(II)_{DP}$ and $ETR(II)_{DP}$ followed the same method as explained above for data obtained with the Mini-PAM.

ETR(I) and ETR(II) *vs.* irradiance curves were fitted according to different models (Jassby and Platt, 1976; Eilers and Peters, 1988) to obtain the maximum ETR ($ETR(I)_{max}$ and $ETR(II)_{max}$), the initial slope of ETR *vs.* irradiance curves ($\alpha_{ETR(I)}$ and $\alpha_{ETR(II)}$) and the saturation irradiance of ETR ($E_{k(ETR(I))}$ and $E_{k(ETR(II))}$).

The technical characteristics of the PAM fluorometers used in this study and those used in previous reports of the same experiment (Stengel et al., 2014; Figueroa et al., 2014a) are presented in Table S1 (Supplementary data section). In addition, the Y(II) data of an inter-calibration exercise among all fluorometers is presented. No significant difference ($p<0.01$) was found among all PAM fluorometers used (Table S1).

Oxygen measurements

The oxygen consumption and production was determined under solar radiation in *closed* UV transparent chambers using OPTODES Fibox 3, (Presens, Nürnberg, Germany). The temperature was maintained at the same level as in the experiment, *i.e.* AT and AT +4°C using refrigerated circulating water. Each measuring chamber contained 0.019 L of seawater

and 20 mg fresh weight of algal biomass. Three replicates were conducted for each nitrogen and carbon treatment on two consecutive days (n=6 per treatment) under each of the two temperature conditions. Net photosynthesis (NP) was determined under solar natural radiation at noon, followed by measurements of respiration (R) in darkness (for 30 min). Gross photosynthesis (GP) was determined as NP+R. Oxygen evolution was expressed in terms of algal area as μmol O_2 m^{-2} s^{-1}.

Statistical analyses

Interactive effects on physiological parameters obtained from the experimental procedures were analysed using Analyses of Variance (ANOVA) (according to Underwood, 1996). After checking for normality, data were tested for homogeneity of variances by the Cochran's test. In the case of the Mini-PAM data (F_v/F_m, ETR_{max}, α_{ETR} and E_k), a Multi-factorial ANOVA was performed including Temperature (Ambient Temperature, AT, and Ambient Temperature +4°C, AT+4°C), Nitrogen (N; Low and High Nitrogen), CO_2 (C; Low and High Carbon) and Time of sampling (M, Morning; N, Noon; E, Evening), all considered fixed crossed factors, and Vessel as a random factor nested in the interaction N x C and crossed with the other two factors. The factor 'Vessel' or their interactions were always not significant ($p > 0.05$) and this factor was thus not included in the final models. In the case of PAR-energy destination data, they were pooled and a linear regression was performed on the averaged data. The data set of the different variables corresponded to two measurement days (n=6). In the case of the Dual PAM data, a one-way ANOVA was conducted, considering the factor treatment with four levels (LCLN, LCHN, HCLN and HCHN) (n=10). When significant differences were detected, *post hoc* tests were performed using Student-Newman-Keuls tests (Underwood, 1996). The significance level was set at 0.05. Pearson correlation coefficients were calculated and tested between physiological variables as; ETR_{max}, NPQ_{max}, F_v/F_m, α_{ETR}, $E_{Y(NO)}$ and $E_{Y(NPQ)}$ (Sigma plot, IBM).

Principal Coordinates Analyses (PCA) were performed to detect patterns among parameters obtained with the Mini-PAM fluorometer, based on Euclidean distance using PERMANOVA+ with PRIMER6 package. PCA analyses were conducted for F_v/F_m, ETR_{max}, and NPQ_{max} considering treatment (4 levels), time (3 levels) and temperature (2 levels). This procedure corresponding to equivalent ordination of a PCA calculates the percentage of variation explained by each axis in the multidimensional scale; the overlay of the vectors on the PCA was performed using Spearman correlation (Anderson et al., 2008).

RESULTS

Fluorescence parameters of PSII using a Mini-PAM fluorometer

Photosynthetic parameters measured at the beginning of the experimental period (*i.e.*, after acclimation time and before the application of any treatment) by the Mini-PAM are presented in Table 1, with values of 0.69 ± 0.03 for F_v/F_m and 1.26 ± 0.62 for NPQ_{max}. E_k was 674 ± 103.77 µmol photons m^{-2} s^{-1}.

Values for F_v/F_m determined after exposure to different levels of CO_2 and nitrate were significantly impacted ($p<0.05$) by the interaction of CO_2 enrichment and time (Table 2), with significant differences through the day: morning, noon or evening (Fig. 2). F_v/F_m significantly decreased at noon due to photoinhibition; and values were higher for thalli under high carbon (HC) than low carbon (LC) condition, in the morning or evening (Fig. 2). F_v/F_m values recorded in the morning and evening were similar, and also increase from initial values (Table 1, Fig. 2).

Maximal electron transport rate (ETR_{max}) as an indicator of photosynthetic capacity was influenced by a significant interaction ($p<0.05$) between C, time and temperature (Table 2, Fig. 3A). At the beginning of the experiment, *U. rigida* displayed the highest ETR_{max} values (37.39 ± 8.76 µmol e^- m^{-2} s^{-1}; Table 1) of the experimental period (Fig. 3A). At ambient temperature, ETR_{max} increased at noon and was higher for samples under LC than under HC (Fig. 3A). At AT+4°C, a similar trend with higher ETR_{max} values at noon was observed (Fig. 3A), although no significant difference was found between LC and HC. At noon, ETR_{max} under LC was also higher at ambient temperature than at AT+4°C (Fig. 3A). After pooling the data (Fig. 3B), ETR_{max} was greater at noon, with the exception of ETR_{max} in HCLN samples. In the evenings, ETR_{max} was significantly lower at HCLN than at LCLN (Fig 3B).

The photosynthetic efficiency (α_{ETR}) was significantly affected by the interaction among C, N and temperature (Table 2). No significant difference was found between C and N treatments at either ambient temperature or AT+4°C (Fig. 3C), except for thalli under HCLN at AT+4°C which reached higher values compared to the other C and N treatments. When data were pooled, α_{ETR} significantly decreased at noon under HCLN treatment and increased in the evening (Fig. 3D).

Photosynthetically saturating irradiance (E_k) of PSII was impacted by different factors such as time, temperature and the interactions between C and N, and between C and time (Table 2). When the data were pooled (Fig. 4), E_k significantly increased at noon

independently of C supply, with higher E_k under HC than LC, whereas the opposite trend was observed in the evening (Fig. 4).

Non-photochemical quenching (NPQ_{max}), as indicator of the energy dissipation, revealed a significant effect ($p<0.05$) of the interaction between CO_2, time and temperature (Table 2, Fig. 5). NPQ_{max} presented a daily pattern that depended on C level, the interaction with N, and on an interactive effect of C, time and temperature (Table 2, Fig. 5). Taking into account this triple interaction, the highest values were detected at noon under LC at both temperatures (Fig. 5). At noon, the increase in C (HC) resulted in a decrease in NPQ_{max} under both temperature treatments. In the evening, HC samples showed a reduction in NPQ_{max} only under increased temperature (Fig. 5). Overall, NPQ_{max} values were generally higher than initial values at the beginning of the experimental period (Table 1).

The Pearson correlations between the different fluorescence parameters measured are shown in Table 3. F_v/F_m was negatively correlated to ETR_{max}, E_k and NPQ_{max} but positively correlated to α_{ETR}. ETR_{max} was positively correlated to both E_k and NPQ_{max}. α_{ETR} was negatively correlated to both E_k and NPQ_{max} and, finally, E_k and NPQ_{max} were also positively correlated. All Pearson correlation coefficients exhibited a significant *p*-value lower than 0.05.

The energy utilized by *U. rigida* during different quenching responses is presented in the Fig. 6. The effective quantum yield represented the smallest fraction of light use under any of the experimental conditions, and the regulated non-photochemical quenching ($E_{Y(NPQ)}$) was the main destination of the energy absorbed in samples under LC treatment (Fig. 6A-D). Moreover, samples under LCLN and increased temperature displayed the lowest capacity of light absorption (close to the maximal amount of 200 μmol photons m^{-2} s^{-1}). When the thalli under HCHN were kept at increased temperature, approximately twice as much light was absorbed, reaching ~400 μmol photons m^{-2} s^{-1} (Fig. 6H). However, based on a comparison of slopes of the three route of energy dissipation, more than 95% of this energy acquired was lost through non-photochemical quenching (Y(NO) and Y(NPQ)). When samples were kept under HCLN, Y(NO) was the main component for energy allocation, and the slopes of $E_{Y(II)}$ indicate that less than 2% of the energy was used effectively for photosynthesis (Fig. 6E-F), regardless of temperature.

The slopes of the curves representing the light energy destined for photochemical and non-photochemical yields the different C and N treatments, were also estimated (Fig. 6). Significant effects of an interaction were found between the availability of N and temperature

(Table4; F=7.6697; p<0.05) on the slopes of energy for the effective quantum yield (Slope $E_{Y(II)}$). The slopes of non-photochemical quenching parameters (E_{YNO} and E_{YNPQ}) were not affected by any interaction among the evaluated factors.

The effective quantum yield was positively correlated to both energy losses ETR_{max} and NPQ_{max} (Table 4); energy conducted to Y(NO) was positively related to the energy associated with other losses Y(NPQ) and ETR_{max}, but negatively correlated to NPQ_{max}. The energy loss corresponding to Y(NPQ) was positively correlated to ETR_{max} and NPQ_{max}. Finally, ETR_{max} and NPQ_{max} were also correlated positively (Table 4).

Electron transport rates and yields of PSI and PSII using the Dual-PAM fluorometer

Values of Y(I) *vs.* Y(II) for all treatments exhibited a direct linear relationship, and Y(I) was always higher than Y(II), under all treatments (Fig. 7A-D). Specific slopes of Y(I) *vs.* Y(II) based on the regression linear model were 0.7421 for LCLN (Fig 7A), 0.8389 for LCHN (Fig. 7B), 0.8032 for HCLN (Fig. 7C) and 0.7893 for HCHN (Fig. 7D), respectively.

The NPQ calculated from the rapid light curve decreased significantly under HCHN (Fig. 8A). By contrast, the rapid light curves of ETR(I) and ETR(II) *vs.* irradiance indicate that the photosynthetic parameters ETR(I) (Fig. 8B) and ETR(II) (Fig. 8C) decreased significantly under this (HCLN) treatment. Generally, significant effects of treatments were observed for $ETR(I)_{max}$ (F=5.763, p<0.05), $ETR(II)_{max(DP)}$ (F=13.1728, p<0.05), as well as PSI and PSII photosynthetic efficiency ($\alpha_{ETR(I)}$, F=3.0739, p<0.05; $\alpha_{ETR(II)(DP)}$, F=5.024, p<0.05). The lowest $ETR(I)_{max}$ and $ETR(II)_{max}$ were reached under HCLN, and the highest under HCHN. The photosynthetic efficiency of PSI decreased under HCLN. E_k values did not present significant differences among the different treatments (p>0.05).

Comparison of ETR_{max} values obtained with different fluorometers

ETR_{max} values at noon under solar radiation were calculated from previously reported data (Stengel et al., 2014; Figueroa et al., 2014a). For Diving-PAM data (based on Stengel et al., 2014), ETR was calculated using reported effective quantum yield, average irradiance at noon in the experimental vessels, the measured absorptance (Table 5) and 0.5 as F_{II} value. For the Monitoring-PAM data (based on Figueroa et al., 2014a), rETR values were used to calculate ETR by multiplying the absorptance data (Table 5). The data of maximal ETR determined by the Mini-PAM and Dual-PAM are presented in the Tables 1 - 5 and Fig. 3).

Regardless of the type of fluorometer used, the highest ETR_{max} measuring through *in vivo* chlorophyll *a* fluorescence related to PSII was consistenly measured under HCHN, and

the lowest under HCLN (Table 5). The ETR_{max} determined from Y(II) measurements *in situ* under solar radiation (Diving-PAM) was higher than ETR_{max} determined in the laboratory from the rapid light curves using red light as actinic light (Mini-PAM). ETR_{max} determined from Y(II) measurement using the Monitoring-PAM was lower than that obtained using the Diving-PAM, although both measurements were conducted under solar radiation (Table 5). Under LC and ambient temperature, ETR_{max} values determined using the Mini-PAM were not significantly different than those determined by the Monitoring-PAM, whereas for the other treatments, ETR_{max} values were higher when using the Monitoring-PAM than the Mini-PAM. In general, ETR_{max} was higher under AT+4^{o}C, except when the measurements were conducted in the laboratory using the Mini-PAM.

Oxygen measurements

The highest gross photosynthesis determined under solar radiation was reached under HCHN, and the lowest under HCLN at both temperatures (Table 5). Gross photosynthesis reached intermediate values under LCLN and LCHN (Table 5). No significant difference was found between N treatments under LC (Table 5). Respiration rate was similar across the different C, N and temperature treatments, except under HCLN at ambient temperature, where a significant decrease occurred compared to the other treatments (Table 5). Under solar radiation (where *in vivo* chlorophyll *a* fluorescence was determined using the Diving-PAM), the lowest ETR_{max} / GP ratio, *i.e.* transport electrons per oxygen produced, was observed under HCHN; the highest ratio was determined for HCLN at both temperatures. This ratio reached intermediate values under LCHN and LCLN (Table 5).

Principal components analyses

Based on Mini-PAM measurements, Principle Component Analysis (PCA) was undertaken for photosynthetic parameters across all treatments (Fig. 9). The first axis of PCA represented 59.1% of the total variation, and the second axis 19.4% of the total variation. The first two dimensions of the PCA based on different photosynthetic responses represented 79.1% of total the variation (Fig. 9). The first axis could be related to a combination of C and N treatments characterized by the highest productivity (ETR_{max}) and photoprotection (NPQ_{max}) indicators. By contrast, the photoinhibition or F_v/F_m responses appears to represent the reverse part of X-axis. The combination of these variables allowed a separation of the treatments revealing that intertidal *Ulva rigida* exhibited responses linked to the C and N treatments.

DISCUSSION

In this study, combined effects of CO_2 and nitrate levels, under two temperature conditions (six days at ambient temperature (AT) followed by three days under AT+4^{o}C) were tested on *Ulva rigida*, an abundant eulittoral Mediterranean green macroalga.

Interactive effects of C, N and temperature

Most studies on the effects of global change factors on aquatic organisms have been conducted using only one or two environmental variables, and studies on the interaction of multiple stressors remain scarce (Cornwall et al., 2012; Koch et al., 2013; Yildiz et al., 2013; Celis-Plá et al., 2017a, b; Gao et al., 2018 and 2019). In this study, we focused on the interactive effects of four variables, *i.e.*, temperature, carbon and nitrogen availability, and time. Little is known about how seaweeds living under nutrient-limited conditions will respond to ocean acidification. In addition, the effect of acidification (as linked to high-CO_2 levels) and nutrient limitation on *Ulva* species is of interest (Rautenberger et al., 2015; Gao et al., 2016; Li et al., 2018) due to their ecological importance, their capability to form green tides (Smetacek and Zingone, 2013), their delivery of crucial ecosystem services such as wastewater bioremediation (Al-Hafedh et al., 2015), and their uses as animal feed (Rico et al., 2016), human food (Yaich et al., 2015), biofuel (Neveusx et al., 2014).

Although young and adult thalli of *Ulva* spp. may display differential responses to ocean acidification and nutrient limitation (Stengel et al., 2014; Figueroa et al., 2014a, c; Gao et al., 2011; Gao et al., 2018), the ability to respond to CO_2 enrichment is generally dependent on ambient N availability (Gordillo et al., 2001; Zou et al., 2011). In coastal areas occupied by *Ulva* spp. including *U. rigida*, ammonia and nitrate concentrations are typically higher due to by urban waste effluents, commonly resulting in the formation of green tides. Corneliesen et al. (2007) showed interactions between physical gradients and nutrient source pools on the N signature of *U. pertusa*, affecting both carbon and nitrogen assimilation. Data from this present study clearly indicate that a decrease in ETR_{max} under elevated CO_2 (HC) occurred only under nitrate limitation (LN). In fact, higher nitrate availability (HN) resulted in a large increase in ETR_{max} not only under HC, but also LC treatments. Under HNLC, the observed high ETR_{max} values in the experimental time were probably transient since the stoichiometry C:N could be affected and ETR_{max} could be reduced by increasing the culture time. Previously, in *Ulva rotundata*, an increase in nitrate supply reduced photoinhibition at noon during daily cycles (Henley et al., 1991b).

Baydend et al. (2010) demonstrated that both ocean acidification and elevated nutrient concentration reduced the growth of coralline crusts, and the combination of these factors led to a further decrease in growth. Elevated pCO_2 reduced net photosynthetic rate under N, P and N-P limitations, but increased nitrate reductase activity and soluble protein content, under P-replete conditions; by contrast, N or P limitation reduced nitrate reductase activity and soluble protein content in *U. linza* (Gao et al., 2018). An increase in CO_2 can enhance the uptake and assimilation of nitrogen in *U. rigida* (Gordillo et al., 2001) and *U. lactuca* (Zou et al., 2001). This would allow a decrease in the energy required for nitrate assimilation due to a release of nitrogen, and any saved available energy can thus be channelled into other processes, such as repair or photoprotection (Zou et al., 2003). In *U. rigida* an increase in photosynthetic rates under HC supply is linked to a stimulation of nitrate reductase activity under high N supply (Gordillo et al., 2001 and 2003) but acidification and nitrate depletion (HCLN) reduced soluble protein level (Figueroa et al. 2014c). In the present study, a decrease in pH and elevated CO_2 levels in the HC treatments lowered the photosynthetic activity and photoprotective capacity in *U. rigida*, probably due to a negative effect on C acquisition, concentration mechanism and energy dissipation processes. *Ulva rigida* uses preferentially bicarbonate when Ci saturated and growth is mainly controlled by light, rather than CO_2 (Rautenberger et al., 2015). These authors concluded that future increased CO_2(aq) levels alone cannot stimulate *Ulva* growth and resultant blooms, and ocean acidification, when combined with increased irradiance, might even suppress green tide blooms. Locally, ocean acidification and nutrient limitation may thus synergistically reduce growth of *Ulva* species and limit the occurrence of green tides in a future ocean environment. Specifically in the coastal area of Malaga (Southern Iberian Peninsula), nitrate concentration are reduced as a consequence of the weakening of wind-induced upwelling; as a result, oligotrophication is becoming more recurrent here (Mercado et al., 2012), and ocean acidification may reduce productivity of *Ulva* species.

The decrease in photosynthetic production (ETR_{max}) under increased temperature observed in this study (when using a Mini-PAM) could be related to a decrease in chlorophyll *a* level previously described by Stengel et al. (2014). A reduced chlorophyll *a* content of *U. lactuca* under elevated (700 ppm) compared to preindustrial (280 ppm) CO_2 levels was also previously reported by Olischläger et al. (2013). Increased temperature also reduced maximum gross photosynthesis and dark respiration in *Ulva pertusa*, and the interaction of elevated carbon and elevated temperature had negative impacts on photosynthesis and biochemical composition (Kang and Kim, 2016). Similar results are also reported in this

study for *U. rigida* relating to ETR_{max}, taking into account the biochemical composition (pigments and proteins) previously described (Figueroa et al., 2014c).

Xu and Gao (2012) reported that growth and ETR of *U. prolifera* was enhanced by elevated CO_2 concentration. However, a reduction in the maximal photosynthetic oxygen evolution rate, the light use efficiency and the efficiency to dissipate excessive light energy was described as Liu et al. (2012) for the same algal species when grown under the same high CO_2 level over a longer period (80 d). Some *Ulva* species exhibit a very high affinity for dissolved inorganic carbon, dominating tidal pools with pH higher than 10.5 (Axelsson et al., 1995). In the present experimental set-up, under LC, pH reached maximal values of pH 9.5-10 (Stengel et al. 2014), corresponding to a CO_2 concentration lower than 1 µM as conditions previously measured in tidal pools (Björk et al., 2004). The conductance for CO_2 together with the uptake of nitrate is high in *U. rigida* (250×10^{-6} m s^{-1}) (Stengel et al., 2014), and it is further thought that *U. rigida* has a high capacity to use bicarbonate and retains high carbonic anhydrase activity compared to other macroalgae (Mercado et al., 1998). *Ulva lactuca* could thus modify the seawater carbonate system via its photosynthetic activity: under a CO_2 pre-industrial treatment (280 ppm), HCO_3^- is incorporated via an anion-exchanger (AE-state) which has the highest affinity for HCO_3^- (Axelsson et al., 1995). Uunder a future scenario of increased CO_2 in rockpools, *Ulva* biomass may increase (Olischläger et al., 2013). Using inhibitors of photosynthetic inorganic carbon utilization, Gao et al. (2016) demonstrated that both extracellular carbonic anhydrase (CA) and intracellular CA were active in *Ulva linza* grown under LC whereas under HC, extracellular CA was completely inhibited. The down-regulated CCMs (Carbon Concentration Mechanisms) in *U. linza* was not affected by changes of seawater carbon chemistry but a decrease in net photosynthetic rate was observed when thalli were exposed to increased light intensity (Gao et al., 2016).

***Fluorescence parameters of PSII and comparison between in-situ* vs. *ex-situ* measurements**

In *U. rigida*, the maximal quantum yield (F_v/F_m) presented a decrease at noon, indicating the presence of photoinhibition. Photoinhibition was higher under LC than under HC treatments, whereas the non-photochemical quenching increased at noon under LC at both temperature treatments, indicating a high capacity for energy dissipation and photoprotection. A decrease in NPQ when more carbon is available has also been demonstrated in microalgae

(Berteotti et al., 2016). In this study, the 4°C increase showed no effect on NPQ_{max}. However, other species, such as the brown macroalga *Fucus serratus*, showed a decrease in NPQ_{max} with increasing temperatures (Figueroa et al., 2019). In contrast to *Ulva* sp., *Fucus serratus* is suffering a decrease in biomass due to climate change (Duarte and Viejo, 2018). A positive temperature dependence of NPQ has been previously reported in vascular plants but when applying a higher temperature increase (+10°C) than in this study (+4°C) (Hendrickson et al., 2004). The high NPQ_{max} values recorded at noon, principally under LC treatment, indicates an effective acclimation of *U. rigida* to high irradiance levels since a high dissipation of energy is related to photoprotection mechanism, which was also observed by Figueroa et al. (2014b) and Stengel et al. (2014) in the same algal species after increased UV-B radiation. A large decrease in F_v/F_m due to an increase of PAR and/or UVR, but also a high capacity of recovery in the evening, has been reported previously for the same species (Figueroa et al. 2003b).

In contrast to $F_v/F_{m,}$ ETR_{max} and E_k increased at noon. Diurnal variations in E_k and ETR have previously been observed in the red macroalga *Kappaphycus alvarezii* (Schubert et al., 2004). The negative relationship between α_{ETR} and ETR_{max} (R=-0.351, $p<0.05$) and between α_{ETR} and E_k (R=-0.735, $p<0.05$) indicated photoacclimation to high light, as respresented by an increase in ETR_{max} and *E*k and decrease in α_{ETR}. Under most conditions, light-saturated photosynthesis (P_{max}) appears to be limited by downstream processes (Behrenfeld et al. 1998) as carbon or nitrogen assimilation. Nitrogen limitation forces photosynthetic organisms to reallocate available nitrogen to essential functions as protein accumulation, enzymatic process and growth. At the same time, it increases the probability of photodamage by limiting the rate of energy-demanding metabolic processes, downstream of the photosynthetic apparatus (Salomon et al., 2013). Thus, the maximal quantum yield (F_v/F_m) but not the maximal photosynthetic capacity (ETR_{max}) was negatively affected by noon irradiance. As defined by Franklin et al. (2003), photoinhibition is a generic outcome of the failure of photoprotection to mitigate photo-inactivation. Photoinhibition has been suggested as a photoprotective mechanism in *Ulva* spp. (Henley et al., 1991a; Figueroa et al., 2003b), and a decrease in F_v/F_m as a consequence of different ambient stress conditions has previously been reported in *Ulva* (Figueroa et al., 2003b; Figueroa et al., 2014b; Li et al., 2018) and other macroalgal species (Celis-Plá et al., 2016).

ETR_{max} in *U. rigida* was affected by temperature but its pattern depended on the measuring system. When measuring Y(II) under solar radiation using a Diving-PAM or a

Monitoring-PAM, ETR_{max} increased under AT+4°C (Stengel et al., 2014; Figueroa et al., 2014a). By contrast, when ETR_{max} was calculated from rapid light curves conducted in this study by a Mini-PAM in the laboratory, it decreased with at the higher temperature. Thus, under *in situ* measurements (natural solar radiation), a different pattern related to growth temperature on ETR_{max} was found. The saturation light pulses of the different fluorometers represent different light qualities, *i.e.* produced by halogen lamp (Diving-PAM), or blue (Monitoring-PAM) or red (Mini-PAM and Dual-PAM) LEDs, but the effect of the light quality on the measuring pattern remains obscure; the observed results may be explained by differences in saturation pulse spectra that could contribute differently affect the electron flow from accessory pigments (carotenoids) to chlorophyll *a* (Celis-Plá et al., 2016).

The energy dissipation pattern was affected by C treatment. Under LC, the main energy loss was produced under regulated photoprotective mechanisms, *i.e.* Y(NPQ), whereas under HC, the main energy loss was passively dissipated as heat, *i.e.* Y(NO). Again, the more favourable treatment for the use of energy for electron transport was HCHN since approximately twice as much light was absorbed, *i.e.*~400 µmol photons m^{-2} s^{-1}, than under the LC treatment. Despite the fact that more than 95% of this energy acquired was lost by non-photochemical quenching (Y(NO) and Y(NPQ)), when comparing the slopes of the three energy destinations, Y(NO) was the main component of energy fate under HCLN; by contrast, Y(NPQ), related to photoregulated energy dissipation mechanisms, was higher under HCHN than under HCLN. The observed differences in energy losses, interestingly, show that the photosynthetic conditions are more favourable under HCHN than HCLN for *U. rigida*.

Similar to ETR_{max}, rates of gross photosynthesis quantified by oxygen evolution were maximal under HCHN, at both temperatures; by contrast, lowest rates were reached under HCLN, which was again similar to observations on ETR_{max}. A good relationship between ETR_{max} (determined under solar radiation using the Diving-PAM) and GP was thus found. However, the ratio of ETR_{max}/GP was far from the expected theoretical values, *i.e.* 4-6 including only PSII (Flameling and Kromkamp, 1998; Figueroa et al., 2003a). This ratio indicates the number of moles of electron transported in the electron transport chain related to the number of moles of oxygen produced. In this study, the ETR_{max}/GP ratio ranged from about 31 to 77, indicating that the algae were not under optimal conditions. The lowest values, related to less stressful physiological conditions, were observed under HCHN, both at AT and AT+4°C (ETR_{max}/GP values: 33.9 and 31.62, respectively), whereas the least

favourable physiological condition was represented by HCLN, at both temperatures (ETR_{max}/GP values: 58.43 and 77.7, respectively). Previously reported values of ETR/C assimilation expressed as mole of electron per mole of C ranged from 5 to 60 and were determined *in situ* for phytoplankton (Lawrenz et al., 2013; Carrillo et al., 2015) and under laboratory conditions for macroalgae (Figueroa et al., 2003a). ETR_{max}/GP values that are higher than 4-6 are reached under unfavourable irradiance, nutrients and temperature conditions and indicate the activation of the alternative electron flow as Mehler reaction, the cyclic electron flow around PSII and/ or PSI, and photorespiration, mechanisms whose activation is probably taxa-specific (Flameling and Kromkamp, 1998; Suggett et al., 2009; Schuback et al., 2016).

In general, the ETR_{max} values in *U. rigida* were higher when Y(II) was determined under solar radiation than under artificial actinic light, as previously reported for *Ulva lactuca* (Longstaff et al., 2002) and the green microalga *Chlorella fusca* (Jerez et al., 2016). A possible explanation is that, under solar radiation, not only chlorophyll but accessory pigments are excited and transfer photons to chlorophyll to a greater extent than that under red actinic artificial light. On the other hand, the ETR_{max} values determined using a Diving-PAM were higher than those determined using a Monitoring-PAM. This result could be explained by the fact that, when using the Monitoring-PAM, the algal thalli were fixed in a clip at 180^{o} angle whereas, when using the Diving-PAM, the algae were free-floating, thus receiving solar radiation from different angles but were also subject to self-shading due to the high algal density in the vessels (27 g FW L^{-1}). Consequently, measured Y(II) was higher when using the Diving-PAM than the Monitoring-PAM system, because in this latter system samples were exposed to higher solar irradiance. The irradiance used to calculate ETR when using the Monitoring-PAM was measured directly next to the algae fixed within the clip, whereas for the Diving-PAM measurements, average irradiances determined at three depths within the vessels were used (surface, 5-cm and 10-cm depth) since algae moved within the water column due to air injection. In the experimental set-up that Diving-PAM measurements were based on, algae were thus subjected to greater light fluctuations than in the Monitoring-PAM system. Similar to our conclusions derived here for *U. rigida*, Longstaff et al. (2002) previously highlighted that *in situ* Y(II) data more realistically related to natural physiological responses than those obtained under the laboratory conditions using artificial actinic light. We thus suggest that ETR measurements *in situ* are more closely related to productivity than ETR measurements *ex situ*. The importance of *in situ* fluorescence measurement on *Ulva* spp.

either in the field or in outdoor tanks, rather than under laboratory conditions, has been previously reported in order to achieve most accurate estimation of algal photosynthesis and productivity (Häder et al., 1999; Altamirano et al, 2000a,b; Cabello-Pasini et al., 2000; Figueroa et al., 2009; Cabello-Pasini et al., 2011). Importantly, the response to experimental variables was consistent across all PAM systems and also when measuring oxygen evoluation, *i.e.* the highest photosynthetic activity observed was under HCHN, and lowest under HCLN.

In vivo *chlorophyll fluorescence of PSII compared to that of PSI*

Another distinct feature among algal species and treatments is the relative contribution of PSI and PSII to photosynthesis. Here, the ETR(I):ETR(II) ratio was about 2.01, and this value was not affected by increased CO_2 or N supply. As a higher activity of PSI has been related to stress conditions (Bukhov and Carpentier, 2004; Gao et al., 2011), in *U. rigida*, PSI could have an important role in the stress acclimation. For example, Gao et al. (2011) reported that the ratio ETR(I):ETR(II) in fully hydrated *Ulva* sp. was 1.35, similar to the lowest values found in *U. rigida* in this study. Under desiccated conditions, this ratio decreased because PSII activity was much more strongly affected by desiccation than that of PSI. In addition, upon rehydration, PSI activity recovered faster than PSII activity (Gao et al., 2011). In our study, changes in the PSII/PSI activity were also related to CO_2 and N supply: under LC conditions, the increase in N enhanced the ETR(I):ETR(II) ratio indicating a higher PSII activity under high N levels. By contrast, under HC conditions, the increase in N resulted in a slight increase in PSI activity. The average value of ETR(II):ETR (I) ratio was 0.54, and thus similar to the ratio reported by Gao and Wang (2012) for *Pyropia yezoensis* under hydrated conditions (0.53). The cyclic electron flow around PSI in the thylakoid membranes has been shown to occur in vascular plants, eukaryotic algae, and cyanobacteria (Ravenel et al., 1994; Mi et al., 1995). During steady-state photosynthesis, cyclic electron flow also contributes to ATP synthesis and adjusts the ATP:NADPH ratio (Backhausen et al., 2000; Kramer et al., 2004b), which is essential for preventing stroma over-reduction (Munekage et al., 2004).

CONCLUSIONS

This study clearly demonstrates that the photosynthetic activity of *U. rigida* decreased under increased CO_2 levels (acidification) but only under N-limitation. Under N-replete conditions, ETR_{max} was higher at elevated CO_2 levels. Following an increase temperature pattern of ETR_{max} observed under different treatments depended on the measuring system and conditions: under solar radiation (*in situ*), ETR_{max} increased with temperature, but in the laboratory under artificial actinic light, no difference or decrease in ETR_{max} with increased temperature was observed. In addition, ETR_{max} was higher when calculated using Y(II) measurements obtained under natural solar radiation than those obtained under artificial light. The activity of PSI was higher than that of PSII under all treatments, and both PSI and PSII activities were reduced under HCLN. This study highlights the importance of 1) research on interactive effects of environmental factors and 2) the measuring approach used (*in-situ vs. ex-situ* conditions) to evaluate the impact of global change on marine macroalgae.

ACKNOWLEDGEMENTS

The financial contributions to the GAP 9 workshop "Influence of the pulsed-supply of nitrogen on primary productivity in phytoplankton and marine macrophytes: an experimental approach" by: Walz GmbH (making available several PAM fluorometers for comparative measurements); Redox; University of Malaga; Ministry of Economy and Competitivity of Spanish Government (Acción Complementaria CTM2011-15659-E); the Project Interacid (RNM5750) of Junta de Andalucía and Spanish Institute of Oceanography are extensively gratefully acknowledged. Paula S.M. Celis-Plá acknowledges partial support from FONDECYT through grant Project FONDECYT N° 11180197, ANID, Chile. Udo Nitschke received financial support from the Marine Institute and the Marine Research Sub-program of the National (Irish) Development Plan 2007-2013. Erik Jan Malta acknowledges funding by the project "The Salty Gold" SIA Foundation, The Netherlands. Francisco Arenas was funded by FCT-Portugal, project Physiography (PTDC/MAR/105147/2008) co-funded by FEDER through the program Compete-Qren. Fungyi Chow thanks the project funding of FAPESP (São Paulo Research Foundation, Brazil). The help of GAP workshop participants with measurements is acknowledged. The measurements of oxygen evolution by Paulina Flores are are thankfully acknowledged.

REFERENCES

Al-Hafedh YS, Alam A, Buschmann AH. 2015. Bioremediation potential, growth and biomass yield of the green seaweed, *Ulva lactuca* in an integrated marine aquaculture system at the Red Sea coast of Saudi Arabia at different stocking densities and effluent flow rates. Reviews Aquaculture 7, 161-171.

Altamirano M, Flores-Moya A, Conde F, Figueroa FL. 2000a. Growth seasonality, photosynthetic pigments and C and N content in relation to environmental factors: a field study on *Ulva olivascens* (Ulvales, Chlorophyta). Phycologia 39, 50 – 58.

Altamirano M, Flores-Moya A, Figueroa FL. 2000b. Long-term effect of natural sunlight under various ultraviolet radiation conditions on growth and photosynthesis of intertidal *Ulva rigida* (Chlorophyceae) cultivated *in situ*. Botanica Marina 43, 119-126.

Anderson M, Gorley RN, Clarke K. 2008. PERMANOVA+ for Primer: Guide to Software and Statistical Methods; PRIMER-e: Plymouth, UK.

Axelsson L, Ryberg H, Beer S. 1995. Two modes of bicarbonate utilization in the marine green macroalga *Ulva lactuca*. Plant Cell Environment 18, 439-445.

Backhausen JE, Kitzmann C, Horton P, Scheibe R. 2000. Electron acceptors in isolated intact spinach chloroplasts act hierarchally to prevent over-reduction and competition for electrons. Photosynthesis Research 64, 1–13.

Baydend R, Joannei T, Lauraj F, Seand C. 2010. Synergistic effects of climate change and local stressors: CO_2 and nutrient driven change in subtidal rocky habitats. Global Change Biology 15, 2153–2162.

Behrenfeld MJ, Prasil O, Kolber ZS, Babin M, Falkowski PG. 1998. Compensatory changes in photosystem II electron turnover rates protects photosynthesis form photoinhibition. Photosynthesis Research 58, 259-268.

Bermejo R, de la Fuente G, Vergara JJ, Hernández I. 2013. Application of the CARLIT index along a biogeographical gradient in the Alboran Sea (European Coast). Marine Pollution Bulletin 77, 107-118.

Berteotti S, Ballottari M. Bassi R. 2016. Increased biomass productivity in green algae by tuning non-photochemical quenching. Scientific Reports 6, 21339.

Bilger W, Schreiber U, Bock M. 1995. Determination of the quantum efficiency of photosystem II and non-photochemical quenching of chlorophyll fluorescence. Oecologia 102, 425-432.

Björk M, Axelsson L, Beer S. 2004. Why is *Ulva intestinalis* the only macroalga inhabiting isolated rockpools along the Swedish Atlantic coast? Marine Ecology Progress Series 284, 109-116.

Brodie J, Williamson C, Smale DA, Kamenos N, Mieszkowska N, Santos R, Cunliffe M, Steinke M, Yesson M, Anderson K, Asnaghi V, Brownlee C, Burdett H, Burrows M, Collins S, Donohue P, Harvey B, Foggo A, Noisette F, Nunes J, Ragazzola F, Raven J, Schmidt D, Suggett D, Teichberg M, Hall-Spencer JH. 2014. The future of the northeast Atlantic benthic flora in a high CO_2 world. Ecology and Evolution 4(13), 2787 - 2798.

Bükov N, Carpentier R. 2004. Alternative photosystem I-drive electron transport routes: mechanisms and function. Photosynthesis Research 82, 17-33.

Cabello-Pasini A, Aquirre-von Webeser E , Figueroa FL. 2000. Photoinhibition of photosynthesis in *Macrocystis pyrifera* (Phaeophyte), *Chondrus crispus* (Rhodophyta) and *Ulva lactuca* (Chlorophyta) in out-door culture systems. Journal Photochemistry Photobiology 57, 169 – 178.

Cabello-Pasini A, Macías-Carranza V, Abdala R, Korbee N, Figueroa FL. 2011. Effect of nitrate concentration on UVR on photosynthesis, respiration, nitrate reductase activity and phenolic compounds in *Ulva rigida* (Chlorophyta). Journal Applied Phycology 23, 363-369.

Caldeira K, Wickett ME. 2003. Anthropogenic carbon and ocean pH. Nature 425, 365-365.

Carrillo P, Medina-Sánchez JM, Herrera G, Duran C, Segovia M, Cortes D, Salles S, Korbee N, Figueroa FL, Mercado JM. 2015. Interactive effect of UVR and phosphorus on the coastal phytoplankton community of the western Mediterranean. Sea: Unravelling eco-physiological mechanisms. PLoS One 10(11), e0142987.

Celis-Plá PSM, Bouzon ZL, Hall-Spencer JM, Schmidt EC, Korbee N, Figueroa FL. 2016. Seasonal changes in photoprotectors and antioxidant capacity of the fucoid macroalga *Cystoseira tamariscifolia*. Marine Environmental Research 115, 89-97.

Celis-Plá PSM, Martínez B, Korbee N, Hall-Spencer JM, Figueroa FL. 2017a. Ecophysiological responses to elevated CO_2 and temperature in *Cystoseira tamariscifolia* (Phaeophyceae). Climatic Change 142, 67-81.

Celis-Plá PSM, Martínez B, Korbee N, Hall-Spencer JM, Figueroa FL. 2017b. Photoprotective responses in a brown macroalgae *Cystoseira tamariscifolia* to increases in CO_2 and temperature. Marine Environmental Research. 130,157-165.

Celis-Plá PSM, Hall-Spencer JM, Horta P, Milazzo M, Korbee N, Cornwall CE, Figueroa FL. 2015. Macroalga responses to ocean acidification depend on nutrient and light levels. Frontiers in Marine Sciences 2(26), 1-12.

Corneliesen CD, Wing SR, Clark KL, Bowman MH, Frew RD, Hurd CL. 2007. Patterns in the δ ^{13}C and δ^{15}N signature of *Ulva pertusa*: Interaction between physical gradients and nutrient source pools. Limnology Oceanography 53, 820-832.

Cornwall CE, Hepburn CD, Pritchard D, Currie KI, McGraw CM, Hunter KA, Hurd CL. 2012. Carbon-use strategies in macroalgae: differential responses to lowered pH and implications for ocean acidification. Journal of Phycology 48, 137-144.

Diffenbaugh S, Pal JS, Giorgi F, Gao X. 2007. Heat stress intensification in the Mediterranean climate change hotspot. Geophysical Research Letters 34, L11706.

Eilers PHC, Peeters JCH. 1998. A model for the relationship between light intensity and the rate of photosynthesis in phytoplankton. Ecological Model 42, 199-215.

Falkenberg LJ, Rusell BD, Connell SD. 2013. Contrasting resource limitations of marine primary producers: implications for competitive interactions under enriched CO_2 and nutrient regimes. Oecologia 17, 575-583.

Figueroa FL, Conde-Álvarez R, Bonomi-Barufi J, Celis-Plá, PSM, Flores P, Malta E.-J, Stengel DB, Meyerhoff O, Pérez-Ruzafa A. 2014a. Monitoring of effective quantum yield in *Ulva rigida* submitted to different CO_2, nutrient and temperature regimes in outdoor mesocosms. Aquatic Biology 22, 195-212.

Figueroa FL, Conde-Álvarez R, Gómez I. 2003a. Relations between electron transport rates determined by pulse amplitude modulated chlorophyll fluorescence and oxygen evolution in macroalgae under different light conditions. Photosynthesis Research 75, 259-275.

Figueroa FL, Dominguez-González B, Korbee N. 2014b. Vulnerability and acclimation to increased UVB in the three intertidal macroalgae of different morpho-functional groups. Marine Environmental Research 97, 30-38.

Figueroa FL, Malta E-J, Bonomi-Barufi J, Conde-Álvarez R, Nitschke U, Arenas F, Mata M, Connan S, Abreu HM, Marquardt R, Vaz-Pinto F, Konotchick T, Celis-Plá P, Hermoso M, Ordoñez G, Ruiz E, Flores P, Kirke D, Chow F, Nassar CAG, Robledo D, Pérez-Ruzafa A, Bañares-España E, Altamirano M , Jiménez C, Korbee N, Bischof K, Stengel DB. 2014c. Short-term effects of increasing CO_2, nitrate and temperature on three Mediterranean macroalgae: biochemical composition. Aquatic Biology 22, 177-193.

Figueroa FL, Israel A, Neori A, Martínez, Malta E-J, Ang P, Inken S, Marquardt R, Korbee N. 2009. Effects of nutrient supply on photosynthesis and pigmentation in *Ulva lactuca* (Chlrophyta): responses to short-term stress Aquatic Biology 7, 173-183.

Figueroa FL, Nygard C, Ekelund N, Gómez I. 2003b. Photobiological characteristics and photosynthetic UV responses in two *Ulva* species (Chlorophyta) from Southern Spain. Journal Photochemical Photobiology 72, 35-44.

Flameling IA, Kromkamp J. 1998. Light dependence of quantum yields for PSII charge separation and oxygen evolution in eukaryotic algae. Limnology Oceanography 43, 284-297.

Figueroa FL, Celis-Plá PSM, Martinez B, Korbee N, Trilla A, Arenas F. 2019. Yield losses and electron transport rate as indicators of thermal stress in *Fucus serratus* (Ochrophyta). Algal Research 41, 101560.

Franklin LA, Osmond CB, Larkum AWD. 2003. UV-B and algal photosynthesis. In: Larkum AWD, Douglas SE, Raven JA, eds. Photosynthesis in algae, advances in photosynthesis and respiration, vol 14. Kluwer Academics Publishers, Dordrecht, 351-384

Gao S, Shen S, Wang G, Niu J, Lin A, Pan G. 2011. PSI-driven cyclic electron flow allows intertidal macroalgae *Ulva* sp. (Chlorophyta) to survey under desiccated conditions. Plant Cell Physiology 52, 885-893.

Gao S, Wang G. 2012. The enhancement of cyclic electron flow around photosystem I improves the recovery of severely desiccated *Porphyra yezoensis* (Bangiales, Rhodophyta). Journal Experimental Botany 63, 4349-4358.

Gao K, Aruga Y, Asada K, Ishihara T, Akano T, Kiyohara M. 1991. Enhanced growth of the red alga *Porphyra yezoensis* Ueda in high CO_2 concentrations. Journal Applied Phycology 3, 355-362.

Gao G, Beardall J, Bao M, Wang C, Ren W, Xu J. 2018. Ocean acidification and nutrient limitation synergistically reduce growth and photosynthetic performances of a green tide alga *Ulva linza*. Biogeosciences 15, 3409–3420.

Gao G, Liu Y, Li X, Feng Z, Xu J. 2016. An Ocean Acidification Acclimatised Green Tide Alga Is Robust to Changes of Seawater Carbon Chemistry but Vulnerable to Light Stress. PLoS ONE 11(12), e0169040.

Gao X, Kim J, Park S, Yu O, Kim Y, Choi H. 2019. Diverse responses of sporophytic photochemical efficiency and gametophytic growth for two edible kelps, *Saccharina japonica* and *Undaria pinnatifida*, to ocean acidification and warming. Marine Pollution Bulletin 142, 315-320.

Genty B, Briantais J-M, Baker NR. 1989. The relationship between the quantum yield of photosynthetic electron transport and quenching of chlorophyll fluorescence. Biochimica et Biophysica Acta 990, 87-92.

Gordillo FJL, Figueroa F, Niell FX. 2003. Photon and carbon use efficiency in *Ulva rigida* at different CO_2 and N levels. Planta 218, 315-322.

Gordillo FJL, Niell FX, Figueroa FL. 2001. Non-photosynthetic enhancement of growth by high CO_2 level in the nitrophilic seaweed *Ulva rigida* C. Agardh (Chlorophyta). Planta 213, 64-70.

Grzymski J, Johnsen G, Sakshaug E. 1997. The significance of intracellular self-shading on the biooptical properties of brown, red and green macroalgae. Journal Phycology 33, 408-414.

Häder DP, Lebert M, Jiménez C, Salles, Aguilera J, Mercado J, Viñegla B, Figueroa FL. 1999. Pulse amplitude modulated fluorescence in the green macrophytes *Enteromorpha muscoides, Ulva rigida, Ulva gigantea and Codium adherens* from the Atlantic coast of Southern Spain. Environmental and Experimental Botany 41, 247-255.

Hall-Spencer JM, Rodolfo-Metalpa R, Martin S, Ransome E, Fine M, Turner SM, Rowley SJ, Tedesco D, Buia MC. 2008. Volcanic carbon dioxide vents show ecosystem effects of ocean acidification. Nature 454, 96–99.

Hendrickson L, Furnbank RT, Chow WS. 2004. A simple alternative approach to assessing the fate of absorbed light energy using chlorophyll fluorescence. Photosynthesis Research 82, 73-81.

Henley WJ, Levavasseur G, Franklin LA, Lindley ST, Ramus J, Osmond CB. 1991a. Diurnal responses of photosynthesis and fluorescence in *Ulva rotundata* acclimated to sun and shade in outdoor culture. Marine Ecology Progress Series 75, 19-28.

Henley WJ, Levavasseur G, Franklin LA, Osmond CB, Ramus J. 1991b. Photoacclimation and photoinhibition in *Ulva rotundata* as influenced by nitrogen availability. Planta 184, 235-243.

Jassby AD, Platt T. 1976. Mathematical formulation of relationship between photosynthesis and light for phytoplankton. Limnology Oceanography 21, 540-547.

Jerez CG, Malapascua JR, Sergejevová M, Masojídek J, Figueroa FL. 2016. *Chlorella fusca* (Chlorophyta) grown in thin-layer cascades: estimation of biomass productivity by *in-vivo* chlorophyll *a* fluorescence monitoring. Algal Research 17, 21-30.

Johnsen G, Sakshaug E. 2007. Biooptical characteristics of PSII and PSI in 33 species (13 different groups) of marine phytoplankton and the relevance for pulse-amplitude-modulated and fast-repetition-rate fluorometry. Journal of Phycology 43, 1236-1251.

Kang EJ, Kim KY. 2016. Effects of future climate conditions on photosynthesis and biochemical component of *Ulva pertusa* (Chlorophyta). Algae 31(1), 49-59.

Klughammer C and Schreiber U. 1994. An improved method, using saturating light pulses, for the deter-mination of photosystem I quantum yield *via* P700+-absorbance changes at 830 nm. Planta 192, 261-268.

Koch M, Bowes G, Ross C, Zhang XH. 2013. Climate change and ocean acidification effects on seagrasses and marine macroalgae. Global Change Biology 19, 103-132.

Kramer DM, Avenson TJ, Edwards GE. 2004b. Dynamic flexibility in the light reactions of photosynthesis governed by both electron and proton transfer reactions. Trends in Plant Science 9, 349–357.

Kramer DM, Johson G, Kiirats O, Edwards GE. 2004a. New fluorescence parameters for the determination of QA redox state and excitation energy fluxes. Photosynthesis Research 79, 209-218.

Kroeker KJ, Kordas RL, Crim RN, Singh GG. 2010. Meta-analysis reveals negative yet variable effects of ocean acidification on marine organisms. Ecological Letters 13, 1419-1434.

Kromkamp JC, Forster RM. 2003. The use of variable fluorescence measurements in aquatic ecosystems: differences between multiple and single turnover measuring protocols and suggested terminology. European Journal Phycology 38, 103-112.

Lawrenz E, Silsbe G, Capuzzo E, Ylostalo P, Forster RM, Simis SGH, Prasil O, Kromkamp JC, Hickman AE, Moore CM, Forget M-H, Geider RJ, Suggett DJ. 2013. Predicting the electron requirement for carbon fixation in seas and oceans. PLoS One 8 (3), e58137.

Li Y, Zhong J, Zheng M, Zhuo P, Xu N. 2018. Photoperiod mediates the effects of elevated CO_2 on the growth and physiological performance in the green tide alga *Ulva prolifera*. Marine Environmental Research 141, 24-29.

Liu Y, Xu J, Gao K. 2012. CO_2-driven seawater acidification increases photochemical stress in a green alga. Phycologia 51, 562–566.

Longstaff BJ, Kildea T, Runcie JW, Cheshire A, Dennison WC, Hurd C, Kana T, Raven JA, Larkum AWD. 2002. An *in situ* study of photosynthetic oxygen exchange and electron transport rate in the marine macroalga *Ulva lactuca* (Chlorophyta). Photosynthesis Research 74, 281-293.

Louanchi F, Boudjakdji M, Nacef N. 2009. Decadal changes in surface carbon dioxide and related variables in the Mediterranean Sea as inferred from a coupled data diagnostic model approach. ICES Journal Marine Science 66, 1538-1546.

Martin S, Gattuso JP. 2009. Response of Mediterranean coralline algae to ocean acidification and elevated temperature. Global Change Biology 15, 2089-2100.

McElhany P, Busch DS. 2013. Appropriate pCO_2 treatments in ocean acidification. Marine Biology 160,1807-1812.

Mercado JM, Cortés D, Ramírez T, Gómez F. 2012. Decadal weakening of the wind-induced upwelling reduces the impact of nutrient pollution in the Bay of Málaga (western Mediterranean Sea). Hydrobiologia 680, 91-107.

Mercado JM, Gordillo FJ. 2011. Inorganic carbon acquisition in algal communities: are the laboratory data relevant to the natural ecosystems? Photosynthesis Research 109, 257-267.

Mercado JM, Gordillo FJ, Figueroa FL, Niell FX. 1998. External carbonic anhydrase and affinity to inorganic carbon in intertidal macroalgae. Journal Experimental Marine Biology and Ecology 221, 209-220.

Mercado J, Jiménez C, Niell FX, Figueroa FL. 1996. Comparison methods for measuring light absorption by algae and their application to the estimation of the package effect. Scientia Marina 60(1), 39-45.

Mi H, Endo T, Ogawa T, Asada K. 1995. Thylakoid membrane bound pyridine nucleotide dehydrogenase complex mediates cyclic electron transport in the cyanobacteria Synechocystis PCC6803. Plant and Cell Physiology 36, 661–668.

Mieszkowska N, Moore P, Hawkins S, Burrows M. 2008. Intertidal Species in Marine Climate Change Impacts. Annual Report Card 2007-2008.

Munekage Y, Hashimoto M, Miyake C, Tomizawa KI, Endo T, Tasaka M, Shikanai T. 2004. Cyclic electron flow around photosystem I is essential for photosynthesis. Nature 429, 579–582.

Neveux N, Yuen AKL, Jazrawi C, Magnusson M, Haynes BS, Masters AF. 2014. Biocrude yield and productivity from the hydrothermal liquefaction of marine and freshwater green macroalgae. Bioresource Technology 155, 334-341.

Ní Longphuirt S, Eschmann C, Russell C, Stengel DB. 2013. Seasonal and species-specific response of five brown macroalgae to high atmospheric CO_2. Marine Ecology Progress Series 493, 91-102.

Olischläger M, Bartsch I, Gutow L, Wiencke C. 2013. Effects of ocean acidification on growth and physiology of *Ulva lactuca* (Chlorophyla) in a rockpool-scenario. Phycological Research 61, 180-190.

Oxborough K, Baker NR. 1997. Resolving chlorophyll a fluorescence images of photosynthetic efficiency into photochemical and non-photochemical components – calculation of qP and *Fv/Fm* without measuring Fo. Photosynthesis Research 54: 135-142.

Pelejero C, Calvo E, Hoegh-Guldberg O. 2010. Paleo-perspectives on ocean acidification. Trends in Ecology and Evolution 25, 332-344.

Platt T, Gallegos CL. 1980. Modeling primary production. In: Falkowski PG, ed. Primary productivity in the sea. Plenum press, New York, 339-362.

Porzio L, Buia MC, Hall-Spencer JM. 2011. Effects of ocean acidification on macroalgal communities. Journal Experimental Marine Biology and Ecology 400, 278-287.

Ramírez T, Cortés D, Mercado JM, Vargas-Yáñez M, Sebastián M, Liger E. 2005. Seasonal dynamics of inorganic nutrients and phytoplankton biomass in the NW Alboran Sea. Estuarine Coastal and Shelf Science 65, 654-670.

Rautenberger R, Fernández PA, Strittmatter M, Heesch S, Cornwall CE, Hurd CL, Roleda MY. 2015. Saturating light and not increased carbon dioxide under ocean acidification drives photosynthesis and growth in *Ulva rigida* (Chlorophyta). Ecology and Evolution 5(4), 874–888.

Raven JA, Ball LA, Beardall J, Giordano M, Maberly SC. 2005. Algae lacking carbon concentrating mechanisms. Canadian Journal of Botany 83, 879-890.

Ravenel J, Peltier G, Havaux M. 1994. The cyclic electron pathways around photosystem I in *Chlamydomonas reinhardtii* as determined in vivo by photoacoustic measurements of energy storage. Planta 193, 51–259.

Rico RM, Tejedor-Junco MT, Tapia-Paniagua ST, Alarcón FJ, Mancera JM, Figueroa FL, Abdala-Díaz RT, Moriñigo MA. 2016. Influence of the dietary inclusion of *Gracilaria cornea* and *Ulva rigida* on the biodiversity of the intestinal microbiota of *Sparus aurata* juveniles. Aquaculture International 24, 965-984.

Riebesell U, Schulz KG, Bellerby RGJ, Botros B, Fritsche P, Meyerhöfer M, Neill C, Nondal G, Oschlies A, Wohlers J, Zöllner E. 2007. Enhanced biological carbon consumption in a high CO_2 ocean. Nature 450, 545-549.

Riebesell U, Zondervan I, Rost B, Tortell PD, Zeebe RE, Morel FMM. 2000. Reduced calcification of marine plankton in response to increased atmospheric CO_2. Nature 407, 364-367.

Roleda MY, Morris JN, McGraw CM, Hurd CL. 2012. Ocean acidification and seaweed reproduction: increased CO_2 ameliorates the negative effect of lowered pH on meiospore germination in the giant kelp *Macrocystis pyrifera* (Laminariales, Phaeophyceae). Global Change Biology 18, 854-864.

Salomon E Bar-Eyal L, Sharon S, Keren N. 2013. Balancing photosynthetic electron flow is critical for cyanobacterial acclimation to nitrogen limitation. Biochimica et Biophysica Acta 1827, 340-347.

Schreiber U, Klughammer C. 2008. New accessory for the Dual PAM 100. The P515/535 module and examples of its application. PAM application notes 1, 1-10.

Schreiber U, Schliwa U, Bilger W. 1986. Continuous recording of photochemical and non-photochemical chlorophyll fluorescence quenching with a new type of modulation fluorometer. Photosynthesis Research 10, 51-62.

Schreiber U, Klughammer C, Neubauer C. 1988. Measuring P700 absorbance changes around 830 nm with a new type of pulse modulation system. Zeitschrift für Naturforschung C 43(9-10), 686-698.

Schuback N, Flecken M, Maldonado M T, Tortell PD. 2016. Diurnal variation in the coupling of photosynthetic electron transport and carbon fixation in iron-limited phytoplankton in the NE subarctic Pacific. Biogeosciences 13, 1019–1035,

Schubert H, Gerbersdorf S, Titlyanov E, Titlyamova T, Granbom M, Pape C, Lüning K. 2004. Circadian rhythm of photosynthesis in *Kappaphycus alvarezii* (Rhodophyta): independence of cell cycle and possible clock. European Journal Phycology 39, 423-430.

Smetacek V, Zingone A. 2013. Green and golden seaweed tides on the rise. Nature 504, 84-88

Sordo L, Santos R, Reis J,Shulika A, Silva J. 2016. A direct CO_2 control system for ocean acidification experiments: testing effects on the coralline red algae *Phymatolithon luisitanicum*. PeerJ 4, e2503.

Stengel DB, Conde-Álvarez R,Connan S, Nitschke U, Arenas F, Abreu MH, Bonomi Barufi J, Chow F, Robledo D, Malta EJ, Mata M, Konotchick T, Nassar C, Pérez-Ruzafa A, López D, Marquardt R, Vaz-Pinto F, Hermoso M, Ruiz E, Ordoñez G, Flores P, Zanolla M, Bañares-España E, Celis Plá P, Korbee N, Bischof K, Figueroa FL. 2014. CO_2, temperature, and nutrient impacts on morphologically different macroalgae under solar radiation: a mesocosm study. Aquatic Biology 22, 159-176.

Suggett DJ, MacIntyre HL, Kana TM, Geider RJ. 2009. Comparing electron transport with gas exchange: parameterising exchange rates between alternative photosynthetic currencies for eukaryotic phytoplankton. Aquatic Microbial Ecology 56, 147–162.

Tyrell T, Schneider B, Charalampopoulou A, Riebesell U. 2008. *Coccolithophores and calcite saturation state in the Baltic and Black Seas.* Biogeosciences 5, 485-494.

Underwood AJ. 1996. Experiments in Ecology: Their Logical Design and Interpretation, using Analysis of Variance. Cambridge University Press, Cambridge.

Villafañe VE, Sundbäck K, Figueroa FL, Helbling EW. 2003. Photosynthesis in the aquatic environment as affected by UVR. In: Helbling EW, Zagarese H, eds. UV effects in aquatic organisms and ecosystems. The Royal Society of Chemistry, Cambridge, 357-397.

Xu J, Gao K. 2012. Future CO_2-induced ocean acidification mediates the physiological performance of a Green Tide Algal. Plant Physiology 160, 1762-1769.

Yaich H, Garna H, Bchir B, Besbes S, Paquot M, Richel A. 2015. Chemical composition and functional properties of dietary fibre extracted by Englyst and Prosky methods from the alga *Ulva lactuca* collected in Tunisia. Algal Research 9, 65-73.

Yildiz G, Hofmann LC, Bischof K, Dere S. 2013. Ultraviolet radiation modulates the physiological responses of the calcified rhodophyte *Corallina officinalis* to elevated CO_2. Botanica Marina 56, 161-168.

Zou D, Gao K, Luo H. 2011. Short- and long-term of elevated CO_2 on photosynthesis and respiration in the marine macroalgae *Hizikia fusiforme* (Sargassaceae, Phaeophyta) grown at low and high nitrogen supply. Journal Phycology 47, 87-97.

Zou DH, Gao KS, Ruan ZX. 2001. Effects of elevated CO_2 concentration on photosynthesis and nutrients uptake of *Ulva lactuca*. Journal Ocean University Qingdao 31, 877-882.

Zou DH, Gao KS, Xia JR. 2003. Photosynthetic utilization of inorganic carbon in the economic brown alga, *Hizikia fusiforme* (Sargassaceae) from the South China Sea. Journal Phycology 36, 1095-1100.

TABLES

Table 1. Photosynthetic parameters (mean ± SD; n = 3) of *Ulva rigida*, using a Mini-PAM fluorometer, under low nitrate (5 µM) and Ambient Temperature (23-26^{o}C), *i.e.* at the beginning of the experiment. F_v/F_m = Maximal quantum yield, ETR_{max} = Maximal electron transport rate, α_{ETR} = Photosynthetic efficiency, E_k = Saturating irradiance of the function ETR *vs.* irradiance and NPQ_{max} = Maximal non-photochemical quenching (relative units).

Variables	***Ulva rigida***		
F_v/F_m (relative units)	0.69	±	0.03
ETR_{max} (µmol electrons m^{-2} s^{-1})	37.39	±	8.76
α_{ETR} (µmol electrons/µmol photons)	0.06	±	0.01
E_k (µmol photons m^{-2} s^{-1})	674.07	±	103.77
NPQ_{max} (relative units)	1.26	±	0.62

Table 2. Multifactorial ANOVA effects on photosynthetic parameters of *Ulva rigida*, using a Mini-PAM fluorometer under different Carbon (C; 700-ppm *vs* 380 ppm), Nitrate (N; 50 µM *vs* 5 µM), Time (Time; morning, noon and evening) and Temperature (Ambient Temperature *vs.* Ambient Temperature +4ºC) conditions. *df*: degree of freedom; *MS*: mean square; *F*: *F*-statistic. The significant differences ($p < 0.05$) are shown in bold.

Variables		**F_v/F_m**			**ETR_{max}**			**α_{ETR}**			**E_k**			**NPQ_{max}**		
Source	*df*	*MS*	*F*	*p*	*MS*	*F*	*p*	*MS*	*F*	*p*	*MS*	*F*	*p*	*MS*	*F*	*p*
C (1)	1	0.00	0.10	0.75	**679.99**	**18.41**	**0.00**	**0.01**	**9.83**	**0.00**	19647.78	1.58	0.21	**5.93**	**65.39**	**0.00**
N (2)	1	**0.01**	**4.73**	**0.03**	**337.62**	**9.14**	**0.00**	0.00	2.13	0.15	31103.05	2.50	0.12	0.01	0.14	0.70
Time (3)	2	**0.18**	**58.53**	**0.00**	**1870.63**	**50.65**	**0.00**	**0.01**	**16.41**	**0.00**	**676810.97**	**54.51**	**0.00**	**4.21**	**46.46**	**0.00**
Temperature (4)	1	0.00	0.05	0.82	**509.14**	**13.79**	**0.00**	0.00	1.02	0.31	**121977.75**	**9.82**	**0.00**	0.15	1.70	0.19
(1) x (2)	1	0.00	0.30	0.59	**682.82**	**18.49**	**0.00**	**0.02**	**20.07**	**0.00**	**217162.79**	**17.49**	**0.00**	**0.62**	**6.83**	**0.01**
(1) x (3)	2	**0.01**	**3.67**	**0.03**	105.40	2.85	0.06	**0.04**	**41.70**	**0.00**	**113945.95**	**9.18**	**0.00**	**0.93**	**10.25**	**0.00**
(1) x (4)	1	0.00	0.03	0.87	120.85	3.27	0.07	0.00	0.46	0.50	1162.41	0.09	0.76	0.01	0.10	0.75
(2) x (3)	2	0.00	0.50	0.61	**238.93**	**6.47**	**0.00**	**0.00**	**4.89**	**0.01**	20009.14	1.61	0.20	0.06	0.64	0.53
(2) x (4)	1	0.00	0.82	0.37	4.44	0.12	0.73	0.00	0.02	0.89	2009.56	0.16	0.69	0.04	0.44	0.51
(3) x (4)	2	0.00	0.65	0.53	111.13	3.01	0.05	0.00	0.56	0.57	36864.16	2.97	0.06	0.02	0.25	0.78
(1) x (2) x (3)	2	0.00	0.08	0.92	**226.18**	**6.12**	**0.00**	**0.01**	**6.03**	**0.00**	11264.93	0.91	0.41	0.00	0.03	0.97
(1) x (2) x (4)	1	0.00	0.64	0.43	0.01	0.00	0.99	**0.00**	**4.98**	**0.03**	14774.77	1.19	0.28	0.24	2.66	0.11
(1) x (3) x (4)	2	0.00	0.93	0.40	**167.01**	**4.52**	**0.01**	0.00	1.01	0.37	13783.34	1.11	0.33	**0.43**	**4.70**	**0.01**
(2) x (3) x (4)	2	0.01	1.78	0.17	46.07	1.25	0.29	0.00	1.34	0.27	7692.08	0.62	0.54	0.01	0.11	0.89
(1) x (2) x (3) x (4)	2	0.00	1.56	0.21	7.30	0.20	0.82	0.00	0.34	0.71	2606.37	0.21	0.81	0.04	0.46	0.63
Residual		0.00			36.93			0.00			12417.36			0.09		

Table 3. Values of Pearson correlations among photosynthetic parameters of *Ulva rigida* (N = 144) using a Mini-PAM fluorometer. The significant differences ($p < 0.05$) are shown in bold.

	ETR_{max}	α_{ETR}	E_k	NPQ_{max}
F_v/F_m	**-0.2678** **p = 0.001**	**0.2104** **p = 0.011**	**-0.3993** **p = 0.000**	**-0.519** **p = 0.000**
ETR_{max}		**-0.247** **p = 0.003**	**0.8004** **p = 0.000**	**0.4757** **p = 0.000**
α_{ETR}			**-0.583** **p = 0.000**	**-0.2546** **p = 0.002**
E_k				**0.4075** **p = 0.000**

Table 4. Values of Pearson correlation among the energy used in photochemistry (Y(II)) as $E_{Y(II)}$, the dissipation or yield losses (Y(NO) and Y(NPQ)) as $E_{Y(NO)}$ and $E_{Y(NPQ)}$, respectively, the maximal electron transport rate (ETR_{max}) and the maximal non photochemical quenching (NPQ_{max}) of *Ulva rigida* for the entire experiment measured using a Mini-PAM fluorometer. The significant differences ($p < 0.05$) are shown in bold.

	$E_{Y(NO)}$	$E_{Y(NPQ)}$	ETR_{max}	NPQ_{max}
$E_{Y(II)}$	**0.4803** **p=0.001**	**0.6505** **p=0.000**	**0.9789** **p=0.000**	**0.392** **p=0.006**
$E_{Y(NO)}$		**0.7988** **p=0.000**	**0.5757** **p=0.000**	-0.2638 p=0.070
$E_{Y(NPQ)}$			**0.7183** **p=0.000**	0.2773 p=0.056
ETR_{max}				**0.3357** **p=0.020**

Table 5. Maximal electron transport rate (ETR_{max}) expressed as μmol electrons m^{-2} s^{-1} calculated from Y(II) measurements with different Pulse Amplitude Modulated (PAM) fluorometers; Diving-PAM, Monitoring-PAM, Mini-PAM and oxygen evolution in *Ulva rigida* exposed to High Carbon (HC, 700 ppm) or Low Carbon; (LC, 380 ppm), combined with High Nitrate (HN, 50 μM) or Low Nitrate (LN, 5 μM) at Ambient Temperature (AT) and Ambient Temperature +4°C (AT +4°C). Gross photosynthesis and respiration are expressed as μmol O_2 m^{-2} s^{-1} as gross photosynthesis and dark respiration. The ratio ETR_{max}/GP under solar radiation (Diving-PAM measurements) and the absorptance measurements are also indicated. The light quality of the actinic light (AL) and the saturation light pulses (SLP) of the different fluorometers are indicated. The different letters indicate significant differences ($p < 0.05$, SNK *post hoc* test).

	Ambient temperature				Ambient temperature +4ºC						
Fluorometer	**LCLN**	**LCHN**	**HCLN**	**HCHN**	**LCLN**	**LCHN**	**HCLN**	**HCHN**	**AL**	**SLP**	**Reference**
Diving PAM	66.4±6.8^{a}	60.1±7.3^{a}	45.6±6.3^{b}	72.2±7.8^{c}	83.2±9.2^{c}	82.7±9.8^{c}	67.3±7.2^{a}	93.3±10.1^{c}	Sun	Halogen	Stengel et al. (2014)
Monitoring PAM	32.9±3.5^{d}	29.6±4.2^{d}	16.2±3.1^{e}	42.2±5.2^{b}	60.6±8.2^{a}	59.1±6.1^{a}	27.3±3.1^{d}	61.3±7.5^{a}	Sun	Blue	Figueroa et al. (2014)
Mini PAM	30.8±3.27^{d}	31.7±3.2^{d}	8.8±1.66^{f}	33.3±6.2^{d}	20.3±3.2^{d}	16.4±2.8^{g}	8.9±2.2^{f}	25.0±1.3^{d}	Red	Red	This study

	Ambient temperature				Ambient temperature +4ºC					
Oxygen measurement	**LCLN**	**LCHN**	**HCLN**	**HCHN**	**LCLN**	**LCHN**	**HCLN**	**HCHN**	**AL**	**Reference**
Gross Photosynthesis	1.59±0.3^{a}	1.46±0.2^{a}	0.78±0.21^{b}	2.13±0.25^{c}	1.80±0.3^{a}	1.70±0.6^{a}	1.20±0.3^{b}	2.95±0.30^{c}	Sun	This study
Respiration	0.49±0.08^{A}	0.42±0.1^{A}	0.24±0.05^{B}	0.39±0.07^{A}	0.49±0.1^{A}	0.34±0.07^{A}	0.31±0.07^{A}	0.48±0.08^{A}	Dark	This study

ETRmax/GP	**LCLN**	**LCHN**	**HCLN**	**HCHN**	**LCLN**	**LCHN**	**HCLN**	**HCHN**	**Reference**
Diving PAM	41.7	41.2	58.43	33.9	45.9	39.5	77.7	31.62	This study

	Ambient temperature				Ambient temperature +4ºC				
Treatments	**LCLN**	**LCHN**	**HCLN**	**HCHN**	**LCLN**	**LCHN**	**HCLN**	**HCHN**	**Reference**
Absorptance	0.5±0.04^{a}	0.41±0.03^{a}	0.33±0.028^{b}	0.45±0.035^{a}	0.53±0.06^{a}	0.47±0.03^{a}	0.42±0.05^{a}	0.51±0.06^{a}	This study

FIGURE CAPTIONS

Figure 1. A and **B**. Map of Spain and site of *Ulva rigida* sampling, *i.e.* La Araña Beach (Málaga, Southern Iberian Peninsula, Spain; LA 36°70'N; LO 4°33'W), photograph of the rocky shores of the eulittoral area; **C.** details of the sampling site in the intertidal location of the species; **D.** photograph of *U. rigida* collected from rocky shores; **E.** photograph of the experimental system where *U. rigida* was cultured in the Experimental center "Grice Hutchinson" in Malaga University (LA 36 ° 66'N; LO 4° 47'W); **F.** detail of the four 1000-L tanks used for circulating freshwater to control the temperature in each Nitrate/Carbon treatment used (1=HCHN, 2=HCLN, 3=LCHN and 4=LCLN). Each tank contained 12 vessels of 14 L; three of these vessels are used for *U. rigida* experiment, and the others contained other algal species (see Stengel et al. 2014); **G.** Detail of the vessel where *Ulva rigida* was cultured.

Figure 2. Maximum quantum yield (F_v/F_m; mean ± SD) in *Ulva rigida*, measured using a Mini-PAM fluorometer, exposed for six days to High Carbon (HC, 700 ppm) or Low Carbon (LC, 380 ppm) level, combined with High Nitrate (HN, 50 μM) or Low Nitrate (LN, 5 μM) concentration during the daytime: morning (M; 7:00-8:00 GMT), noon (N;11:30-12:30 GMT) and evening (E; 17:00-18:00 GMT). Data represent the pooled results (n=24) in accordance with significant effects obtained by an ANOVA (Table 2). The different letters indicate significant differences among treatments ($p < 0.05$, SNK *post hoc* test).

Figure 3. A) and B) Maximum electron transport rates (ETR_{max}; mean ± SD, n=12), and **C) and D)** Photosynthetic efficiency (α_{ETR}; mean ± SD; C, n=18 and D, n=12) in *Ulva rigida*, measured using a Mini-PAM fluorometer, exposed for six days to High Carbon (HC, 700 ppm) or Low Carbon (LC, 380 ppm) level, combined with High Nitrate (HN, 50 μM) or Low Nitrate (LN, 5 μM) concentration at Ambient Temperature (AT) *vs.* Ambient Temperature +4°C (AT+4°C) during the daytime: morning (M; 7:00-8:00 GMT), noon (N;11:30-12:30 GMT) and evening (E; 17:00-18:00 GMT). Data represent the pooled results in accordance with significant effects obtained by an ANOVA (Table 2). The different letters indicate significant differences among treatments ($p < 0.05$, SNK *post hoc* test).

Figure 4. Photosynthetic saturating irradiance (E_k; mean ± SD) in *Ulva rigida*, measured using a Mini-PAM fluorometer, exposed for six days to High Carbon (HC, 700 ppm) or Low Carbon;(LC, 380 ppm) level, combined with High Nitrate (HN, 50 µM) or Low Nitrate (LN, 5 µM) concentration at a temperature increased by +4°C during the day: morning (M; 7:00-8:00 GMT), noon (N; 11:30-12:30 GMT) and evening (E; 17:00-18:00 GMT). Data represent the pooled results (n=24) in accordance with significant effects obtained by an ANOVA (Table 2). The different letters indicate significant differences among treatments ($p < 0.05$, SNK *post hoc* test).

Figure 5. Maximum non-photochemical quenching (NPQ_{max}; mean ± SD; n = 12) in *Ulva rigida*, measured using a Mini-PAM fluorometer, exposed for six days to High Carbon (HC, 700 ppm) or Low Carbon (LC, 380 ppm) level, combined with High Nitrate (HN, 50 µM) or Low Nitrate (LN, 5 µM) concentration at Ambient Temperature (AT) *vs.* Ambient Temperature +4°C (AT+4°C) during the daytime: morning (M; 7:00-8:00 GMT), noon (N; 11:30-12:30 GMT) and evening (E; 17:00-18:00 GMT). Data represent the pooled results in accordance with significant effects obtained by an ANOVA (Table 2). The different letters indicate significant differences among treatments ($p < 0.05$, SNK *post hoc* test).

Figure 6. Absorbed PAR energy destined to different photochemical routes in *Ulva rigida* (mean of n=6), using a Mini-PAM fluorometer: *i.e.* PAR-energy to effective quantum yield ($E_{Y(II)}$), PAR-energy to non-regulated non-photochemical quenching ($E_{Y(NO)}$), and PAR-energy to regulated non-photochemical quenching ($E_{Y(NPQ)}$), under High Carbon (HC, 700 ppm) or Low Carbon (LC, 380 ppm) level, High Nitrate (HN, 50 µM) or Low Nitrate (LN, 5 µM) concentration in combination with Ambient Temperature (AT) *vs.* Ambient Temperature +4°C (AT+4°C). **A)** LCLN under AT, **B)** LCLN under AT+4°C, **C)** LCHN under AT, **D)** LCHN under AT+4°C, **E)** HCLN under AT, **F)** HCLN under AT+4°C, **G)** HCHN under AT, and **H)** HCHN under AT+4°C. Regression linear equations are included.

Figure 7. Correlation between Y(I) and Y(II) in *Ulva rigida*, according to four treatments; **A)** LCLN (Low Carbon, 380 ppm and Low Nitrogen, 5 µM), **B)** LCHN

(Low Carbon, 380 ppm and High Nitrate, 50 μM), **C)** HCLN (High Carbon, 700 ppm and Low Nitrate, 5 μM) and **D)** HCHN (High Carbon, 700 ppm and High Nitrogen, 50 μM). Measurements were performed using a Dual PAM fluorometer. The algae were exposed either at Ambient Temperature (AT) or Ambient Temperature +4°C (AT+4°C) for each treatment (n=140).

Figure 8. Rapid light curves for *Ulva rigida* cultivated in four combinations of nitrate and carbon availability, using a Dual PAM fluorometer, of **A)** Non-photochemical quenching (NPQ), **B)** Electron transport rate of PSI (ETR(I)), and **C)** Electron transport rate of PSII (ETR(II)) *vs.* irradiance.

Figure 9. *Ulva rigida*. Principal Components (PC) diagrams in relation to photosynthetic data obtained using a Mini-PAM fluorometer according to four treatments; LCLN (Low Carbon, 380 ppm and Low Nitrate, 5 μM), LCHN (Low Carbon, 380 ppm and High Nitrate, 50 μM), HCLN (High Carbon, 700 ppm and Low Nitrate, 5 μM) and HCHN (High Carbon, 700 ppm and High Nitrate, 50 μM).. Vector overlay (Sperman rank correlation) indicates the relationship between the PC1 and PC2 axes and the physiologycal variables as; F_v/F_m (maximal quantum yield), ETR_{max} (maximal electron transport rate), and NPQ_{max} (maximal non- photochemical quenching).

Figure 1

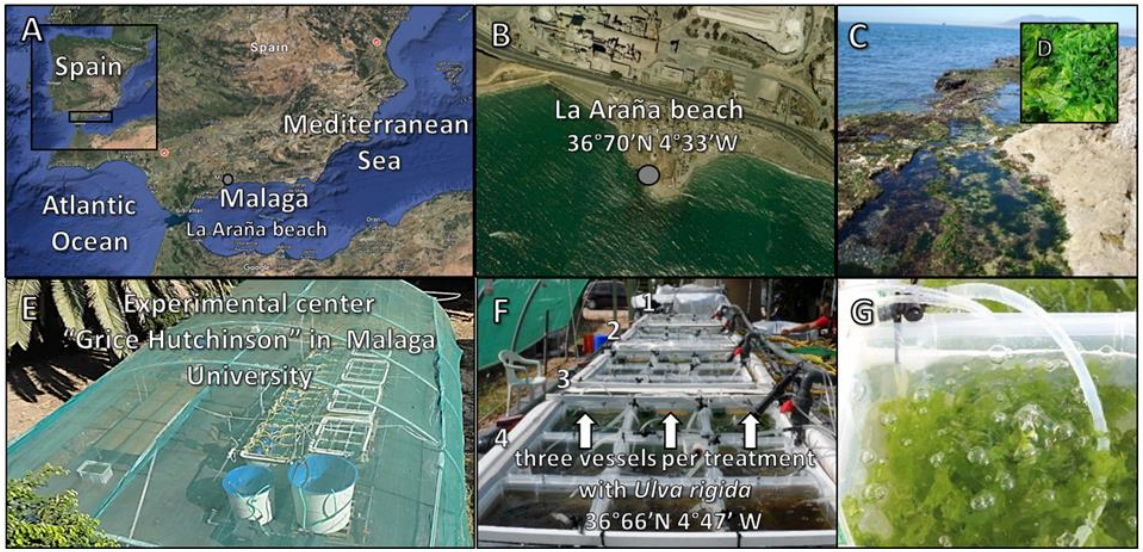

Figure 2

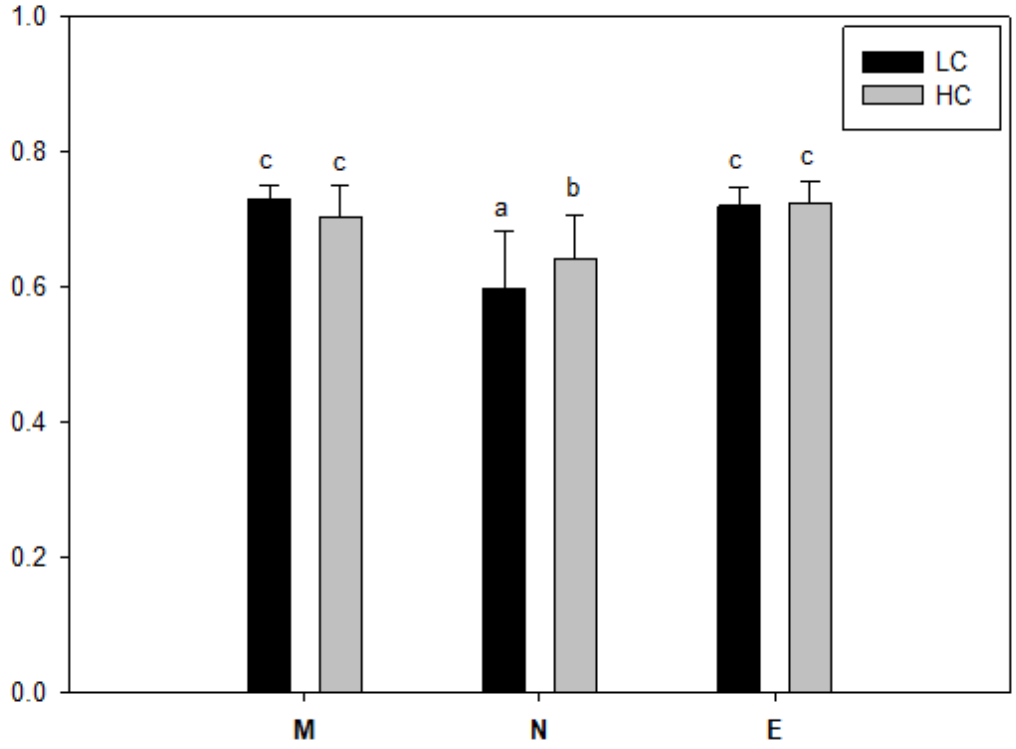

Figure 3

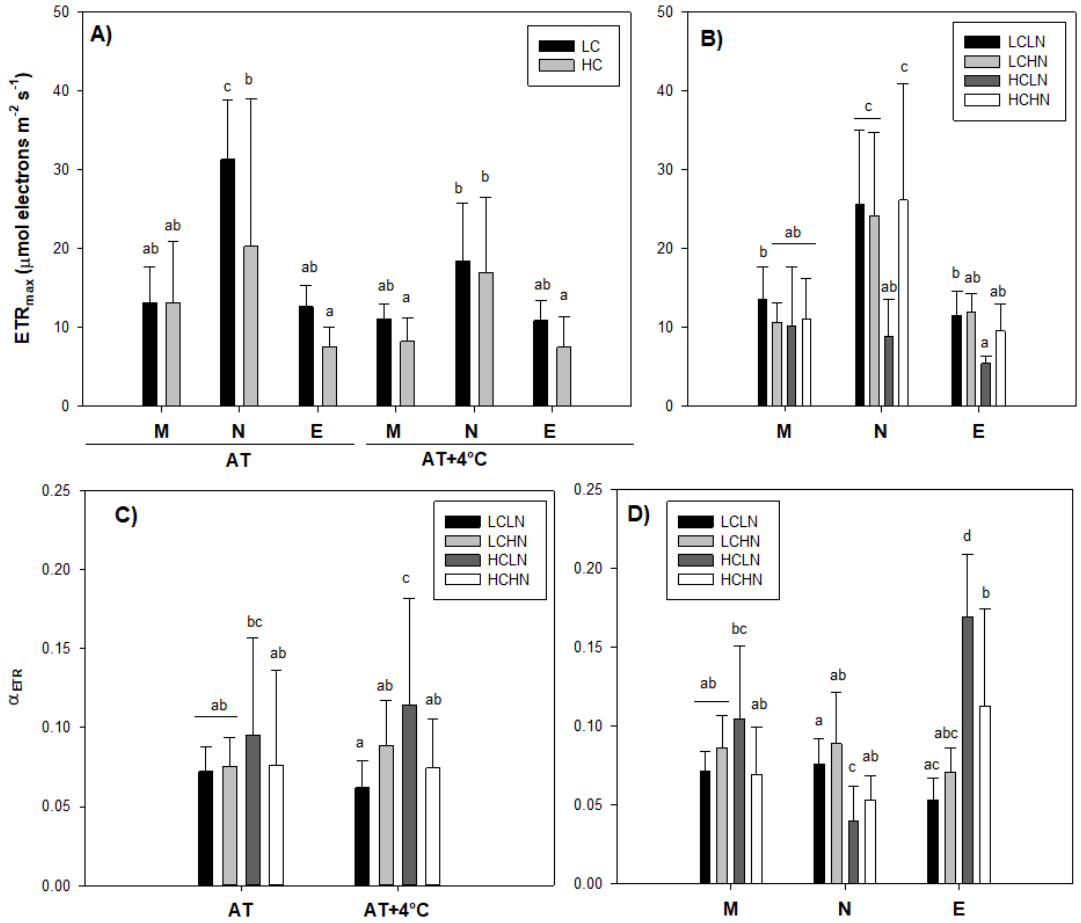

Figure 4

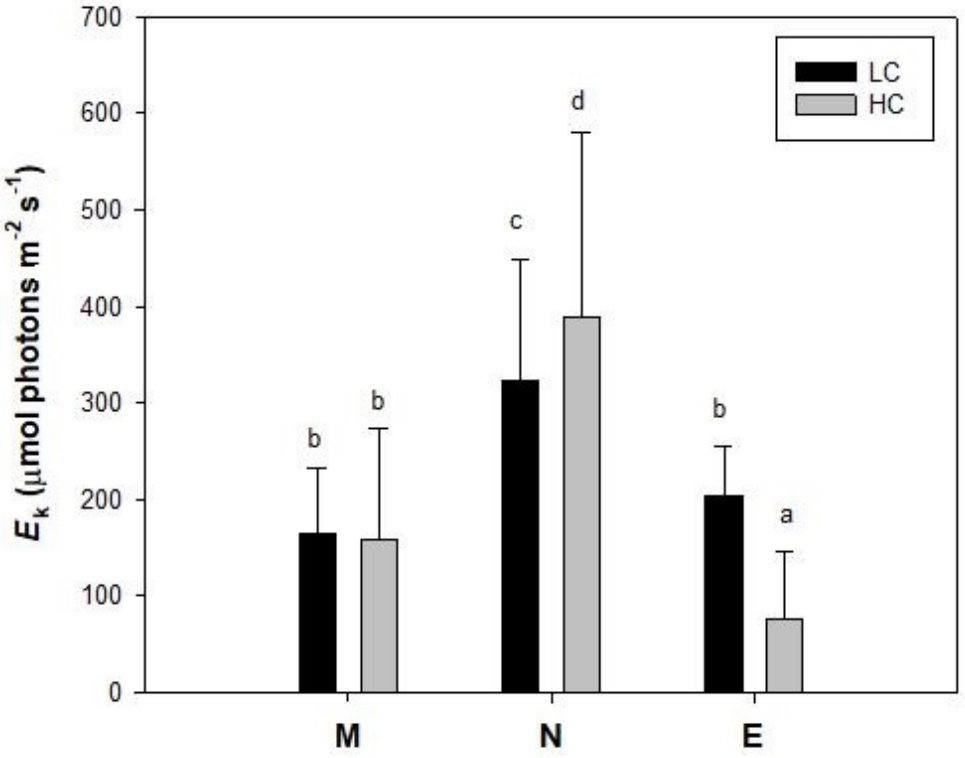

Figure 5

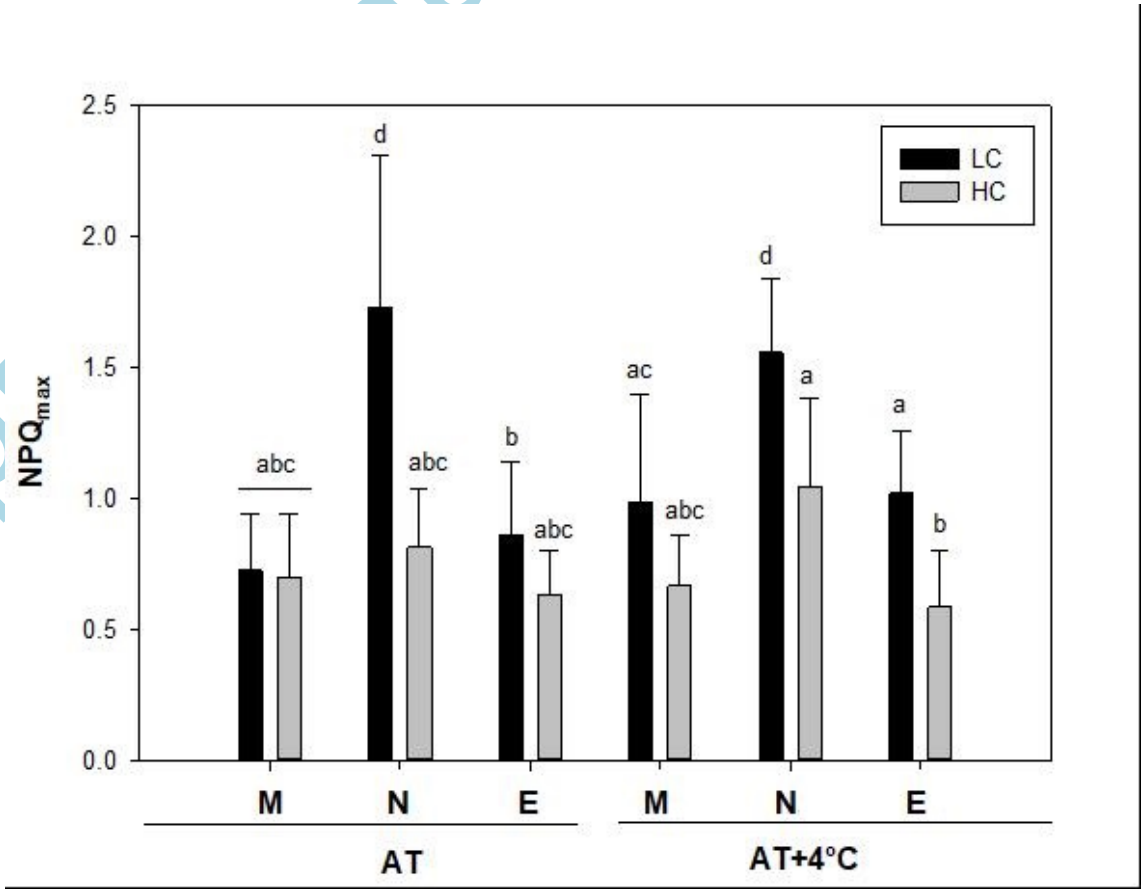

Figure 6

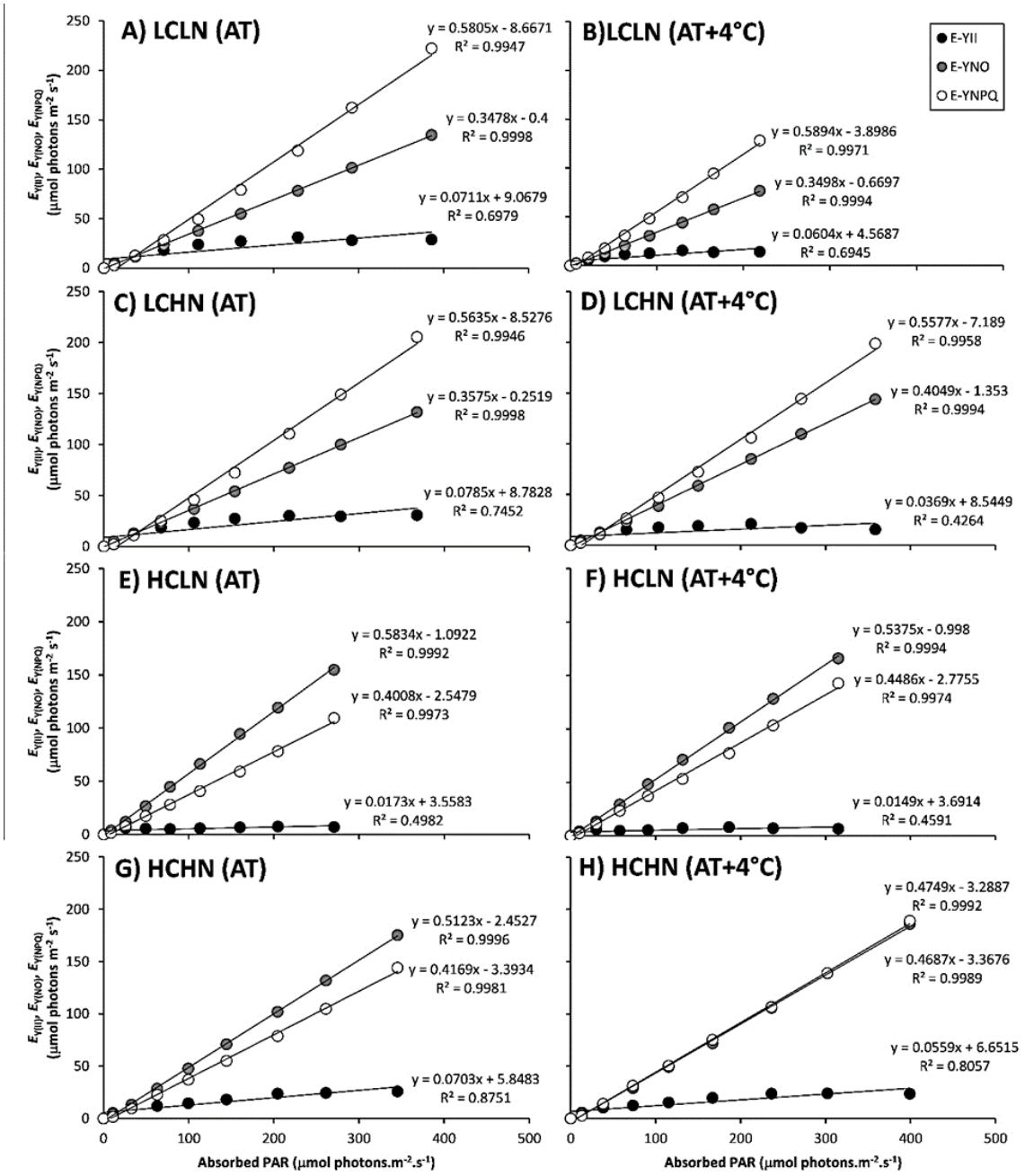

Figure 7

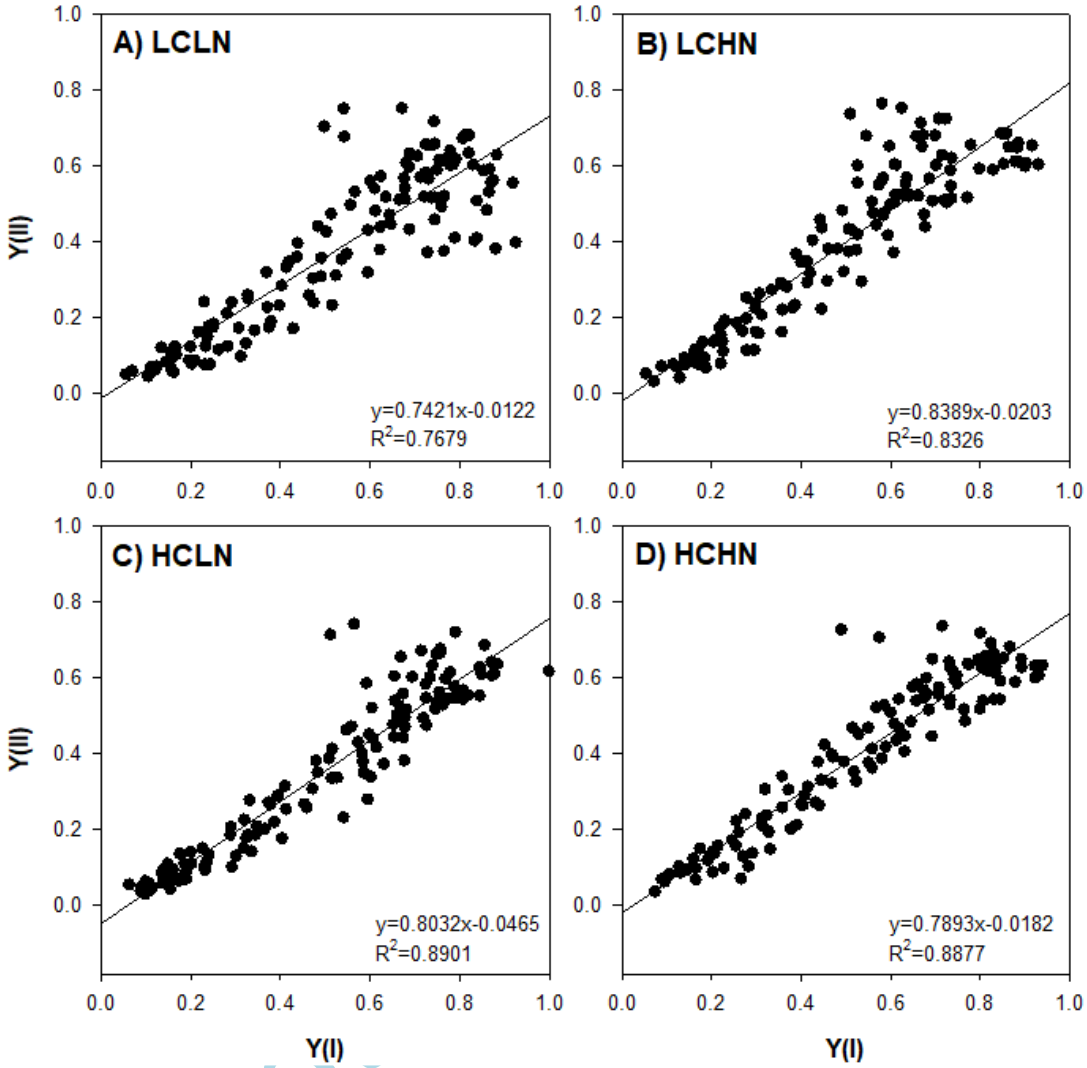

Figure 8

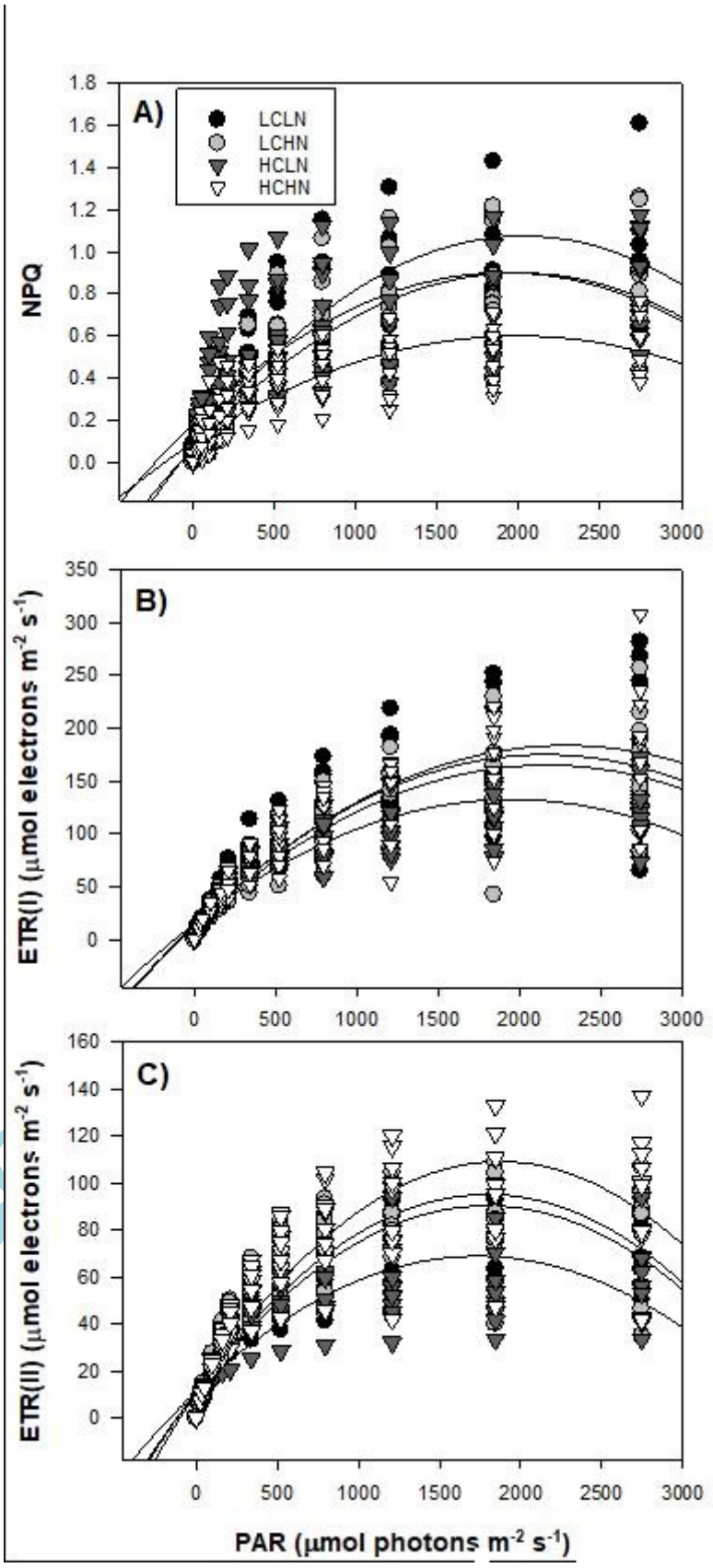

Figure 9